



# Artificial Organelles: Towards Adding or Restoring Intracellular Activity

Roy A. J. F. Oerlemans<sup>+, [a]</sup>, Suzanne B. P. E. Timmermans<sup>+, [a]</sup> and Jan C. M. van Hest<sup>\*, [a]</sup>



Compartmentalization is one of the main characteristics that define living systems. Creating a physically separated micro-environment allows nature a better control over biological processes, as is clearly specified by the role of organelles in living cells. Inspired by this phenomenon, researchers have developed a range of different approaches to create artificial organelles: compartments with catalytic activity that add new function to living cells. In this review we will discuss three complementary lines of investigation. First, orthogonal chemistry approaches are discussed, which are based on the

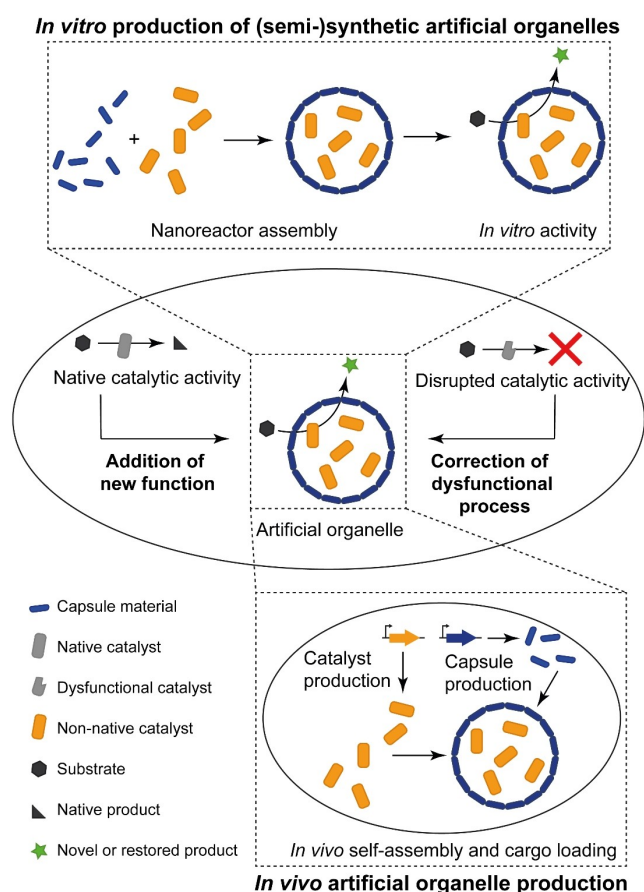
incorporation of catalytically active transition metal-containing nanoparticles in living cells. The second approach involves the use of premade hybrid nanoreactors, which show transient function when taken up by living cells. The third approach utilizes mostly genetic engineering methods to create bio-based structures that can be ultimately integrated with the cell's genome to make them constitutively active. The current state of the art and the scope and limitations of the field will be highlighted with selected examples from the three approaches.

## 1. Introduction

Organelles are essential compartments in living cells. The presence of a physical boundary between the inner and outer environment of an organelle allows nature a higher level of control over a range of crucial biological processes. Organelles provide protection of fragile components, they enable the creation of local microenvironments or chemical gradients and they contribute to positional assembly and enrichment of catalytic species to ensure that processes proceed with greater efficacy. Organelles, such as the cell nucleus and mitochondria, are traditionally thought to be composed of (multiple) lipid bilayer membranes, and are ubiquitous in eukaryotic cells. The similarity in membrane structure between organelles and the cell membrane has been the basis for the theory of endosymbiosis, popularized by Margulis.<sup>[1]</sup> According to this theory, the microbial ancestors of mitochondria and chloroplasts have been internalized by other microbes to ensure the symbiont an autonomous energy supply. This theory has been further strengthened by the discovery of the presence of mitochondrial DNA, which indicates that this organelle originated from an independent life form.

Our classification of organelles has been extended in recent years. First of all it has been shown that membrane-less compartments are present in eukaryotes, which are formed by coacervation of intrinsically disordered proteins, leading to the enrichment of specific biomolecules in this compartment.<sup>[2,3]</sup> Furthermore, organelles are not only to be found in eukaryotes. Prokaryotes also contain organelles, of which the compartment structure is often protein-based, such as is the case with carboxysomes and the propane-1,2-diol utilization (Pdu) microcompartment.<sup>[4,5]</sup>

Besides these organelle structures, nature also employs other methods to attain control over biological processes. The formation of catalytically active protein complexes such as the nonribosomal peptide synthetase, or the usage of scaffolding proteins are approaches often encountered in cells.<sup>[6,7]</sup> It allows different proteins to be arranged in a spatially well-defined manner; this facilitates regulatory mechanisms and even offers control over the sequence of reaction steps. This approach has



**Figure 1.** Schematic overview of the different strategies used for artificial organelle production and integration with living systems. Artificial organelles that are (partially) composed of synthetic components (top) cannot be produced biosynthetically and are thus produced *in vitro* and then introduced to living cells. These organelles will be discussed in Sections 2 and 3. The second class of artificial organelles (bottom) consists of building blocks that can be genetically encoded and can thus be produced *in cellulo* or *in vivo*. This class of artificial organelles will be reviewed in Section 4.

[a] R. A. J. F. Oerlemans,<sup>+</sup> S. B. P. E. Timmermans,<sup>+</sup> Prof. Dr. J. C. M. van Hest  
Bio-Organic Chemistry Research Group  
Institute for Complex Molecular Systems  
Eindhoven University of Technology  
P.O. Box 513 (STO3.41), 5600 MB Eindhoven (The Netherlands)  
E-mail: j.c.m.v.hest@tue.nl

[†] These authors contributed equally to this work.

This article is part of a Special Collection on Xenobiology. To view the complete collection, visit our homepage

© 2021 The Authors. ChemBioChem published by Wiley-VCH GmbH. This is an open access article under the terms of the Creative Commons Attribution Non-Commercial License, which permits use, distribution and reproduction in any medium, provided the original work is properly cited and is not used for commercial purposes.

also been elegantly used by synthetic biologists by constructing *in cellulo* artificial hubs, based on proteins with multiple binding motifs or by using DNA origami scaffolds.<sup>[8]</sup> This work will however not be discussed in detail in this review, as it lacks the confinement aspects characteristic for organelles.

The interesting features of organelles and their importance in biology have inspired many scientists to construct synthetic analogues. Artificial organelle research is directed to the construction of, mostly, catalytically active nanosized compartments that can be integrated with living cells. The purpose of this integration is to either replace or correct dysfunctional processes, or to add novel, orthogonal functionalities to living cells. The former line of application is closely related to the field of nanomedicine, in which a more sophisticated form of enzyme replacement therapy is envisaged, in particular to treat metabolic diseases. Artificial organelles are also used to activate compounds (prodrugs) in targeted cells, to realize a very selective treatment modality. This approach is mainly employed in anticancer therapy.<sup>[9]</sup>

The addition of novel function to living cells is less explored and also more challenging, as functional orthogonality and compatibility are far from trivial to be achieved inside the complex cellular medium. Two approaches can be distinguished; in one approach organelles are transplanted from one organism to the other. This is for example achieved by incorporating chloroplasts in mammalian cells.<sup>[10]</sup> In a second approach a fully artificial organelle, both with respect to membrane structure and catalytic function is created and integrated within the cellular environment. Both approaches, but in particular the former, can be regarded as a form of artificial endosymbiosis.

In this review we will report on two classes of artificial organelles to add novel functionality to living cells. (Figure 1). The first class that will be discussed are (partially) composed of synthetic components which cannot be produced biosynthetically. We hereby make a distinction between two types of nanoreactors. First, we describe the development of bio-orthogonal catalytic processes based on organometallic catalysts which are incorporated in living cells, with a focus on nanoparticulate structures. Secondly, we will discuss hybrid artificial organelles. We will only describe in detail those examples which are truly integrated in living cells or are investigated in cellular medium, such as cell lysate.<sup>[11]</sup> For this class of artificial organelles, the compartments have to be constructed first and then incorporated in living cells via for example endocytosis. This makes this class of artificial organelles also transient in nature: function will be lost and cannot be restored by the cell itself. This is in contrast to the second class of artificial organelles that are composed of building blocks which can also be genetically encoded. These, mostly protein-based compartments can either be produced externally and taken up by cells, or they can be produced *in cellulo*. In that case, the artificial organelles will become a constitutive part of the cellular make up. Rather than trying to be comprehensive, we would like to show the most recent accomplishments in research and we will also highlight the different types of challenges that are still ahead for these classes of nanoreactors, demonstrating their scope and limitations.



Roy Oerlemans received his M.Sc. in molecular life sciences from Radboud University in 2015. During his studies he worked on enzyme-activatable cell-penetrating peptides under the supervision of Prof. Jan van Hest (Radboud University) and on leucine zipper-fused proteins under the supervision of Prof. Ger Pruijn (Radboud University). Thereafter, he worked in the pharmaceutical industry on the design and optimization of scalable synthesis routes for pharmaceuticals and nanomedicines. Currently he is a Ph.D. candidate working on synthetic artificial organelles under the supervision of Prof. Jan van Hest.



Suzanne Timmermans received her M.Sc. in molecular life sciences from Radboud University in 2016. During her studies she worked on 3D human mesenchymal stem cell culture under the supervision of Prof. Wilhelm Huck (Radboud University), *in situ* activatable cell-penetrating peptides under the supervision of Prof. Jan van Hest (Radboud University) and on a glycosyltransferase with expanded sugar substrate specificity under the supervision of Prof. Carolyn Bertozzi (Stanford University). Currently, she is a Ph.D. candidate working on protein nanocage-based artificial organelles under the supervision of Prof. Jan van Hest.



Jan van Hest obtained his Ph.D. from Eindhoven University of Technology (TU/e) in 1996 with Prof. E.W. Meijer. In 2000 he was appointed full professor at Radboud University Nijmegen. Since September 2016, he has held the chair of Bio-organic Chemistry at TU/e, and since May 2017 he has been the scientific director of the Institute for Complex Molecular Systems (ICMS). The group's focus is to develop well-defined compartments for nanomedicine and artificial cell research, using a combination of techniques from polymer science to protein engineering.

## 2. Transition Metal-Based Nanoreactors in Living Cells

Organometallic catalysis has evolved to be a crucial toolbox for organic synthesis over the years. The chemical versatility is large and reactions can be catalyzed that are not to be found in living systems. As such, much attention has been given over the past decade to investigate the possibilities to introduce this type of catalysis in living cells, to perform chemistry orthogonal to natural processes, for example by labeling of cellular components or the localized activation of prodrugs.<sup>[12–16]</sup> Transition metals are naturally present, particularly as co-factors in enzymes, in which they play a key role in their catalytic activity, mostly as Lewis acids or electron-transfer agents.<sup>[17,18]</sup> However, this doesn't imply that transition metal catalysis is easily translated to the cellular environment. This type of catalysis is mostly applied in organic solvents and at elevated temperatures; translation to the fixed conditions of the intracellular environment is thus far from trivial. The complexes need to be air- and water-stable and should be sufficiently active at physiological temperatures. Another challenge is to maintain catalytic activity in the extremely crowded environment of the cell with high concentrations of thiols and amines, which are often poisonous to the catalyst complexes and can even completely inhibit their activity. Furthermore, many transition metal complexes are known to have chemotherapeutic properties. Their mode of action varies from DNA intercalation, disturbance of the cell's redox balance (either by causing oxidative stress or reductive stress) to enzyme inhibition.<sup>[19]</sup> A delicate balance is therefore necessary between stability and activity, preventing interference with or by biological components; in other words, bio-orthogonality is required.<sup>[20,21]</sup> In this section we will focus on intracellular catalysis promoted by organometallic complexes (Table 1). We will first describe catalyst development for the main types of metals used, followed by nanoparticle delivery strategies to facilitate intracellular delivery and activity.

### 2.1. Ruthenium-mediated intracellular catalysis

Ruthenium has become one of the key players in organometallic catalysis.<sup>[49,50]</sup> Its eminent catalytic power stems from its property to adopt a large range of oxidation states, resulting in the development of a vast amount of complexes. Besides its high versatility in catalytic transformations, it has good tolerance to air, water and functional groups, depending on the nature of the complex. It is therefore not surprising that its activity has been examined in more complex media. Thiols, which are abundantly present in the intracellular milieu, however, have often been associated with catalyst poisoning due to their strong coordinating properties. Nevertheless, [Cp\*Ru(cod)Cl] was found to catalyze the allylation of thiols in organic solvent.<sup>[51]</sup> This led to the first abiotic organometallic catalyzed reaction inside live cells by Streu and Meggers.<sup>[22]</sup> Ruthenium complex [Cp\*Ru(cod)Cl] was demonstrated to

deprotect bis-allylcarbamate caged rhodamine (alloc-R110) in the presence of cell extract supplemented with millimolar concentrations of glutathione (GSH) to give rise to green fluorescence (Table 1, entry 1). The presence of the stronger nucleophile thiophenol (PhSH), boosted the reaction yield to 80%. HeLa cells were treated with the probe, washed and incubated with catalyst and thiophenol to afford a tenfold increase in fluorescence.

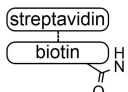
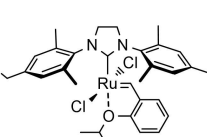
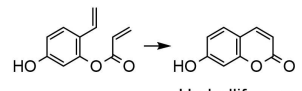
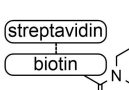
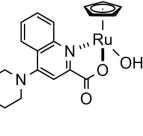
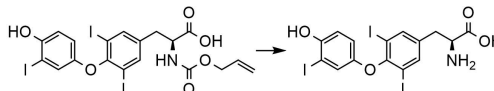
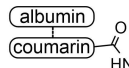
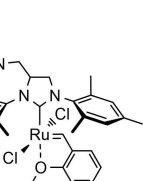
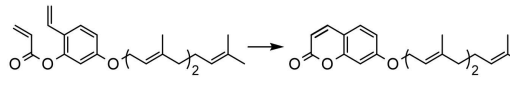
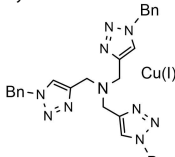
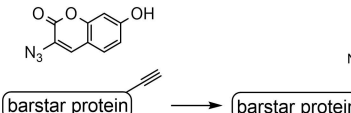
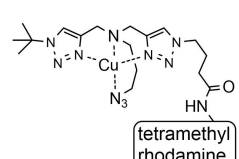
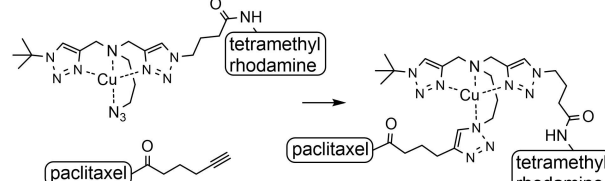
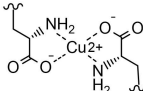
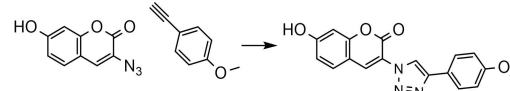

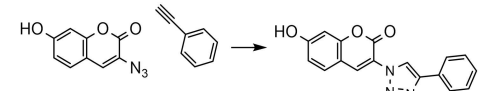

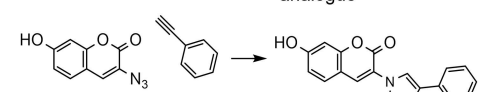
The same approach was used by Mascareñas et al. to uncage DNA staining agents.<sup>[23]</sup> Incubation of chicken embryo fibroblast (CEF) cells with an ethidium bromide based probe showed in first instance green fluorescence mainly localized in the cytosol. After treatment with catalyst and PhSH, fluorescence mainly originated from the nucleus and furthermore, the emission changed from green to red (Table 1, entry 2).

More recently, Meggers et al. reported about a more efficient ruthenium catalyst for the cleavage of carbamates in cells.<sup>[25]</sup> They made use of a ruthenium complex equipped with derivatives of 2-quinolinecarboxylate [CpRu(QA)(allyl)]<sup>+</sup>, developed by Kitamura et al.<sup>[52]</sup> This complex was employed for the uncaging of alloc-R110 in HeLa cells to obtain increased fluorescence intensities of 70- to 130-fold (Table 1, entry 4). This transformation was also used in a prodrug strategy. Doxorubicin caged with an alloc group was introduced into HeLa cells, which were subsequently incubated with the catalyst with an 8-hydroxyquinolate ligand. With this highly active catalyst IC<sub>50</sub> values nearly that of free DOX were reached. Intracellular conversion was not specifically investigated.<sup>[53]</sup>

Going one step further than general intracellular catalysis, complexes were directed to a specific organelle for intracellular targeted catalysis. To this end, Mascareñas et al. tailored [CpRu(QA)(allyl)]<sup>+</sup> with a triphenylphosphonium group for mitochondrial targeting (Table 1, entry 5).<sup>[26]</sup> HeLa and A549 cells were treated with this tagged catalyst, prior to incubation with the alloc-R110 probe. The resulting fluorescent signal colocalized with a mitochondrial tracker. One of the phenyls of the triphenylphosphonium moiety was then replaced by a 1-methylpyrenyl group, a blue fluorescent dye, to be able to observe co-localization of catalyst, rhodamine 110 and mitochondrial tracker. This unambiguously demonstrated that the reaction occurred intracellularly.

Previous examples all involved free complexes which entered cells because of their hydrophobicity, enabling them to pass the cell membrane. Compartmentalization approaches have also been applied, although the number of examples is more limited. Gold nanoparticles were coated with a hydrophobic layer to enable encapsulation of either [Cp\*Ru(cod)Cl] or 1,1'-bis(diphenylphosphino)ferrocene)palladium(II)dichloride (Figure 2).<sup>[24]</sup> The periphery of the coating was functionalized with dimethylbenzylammonium groups, binding partners of cucurbituril[7]. Complexation with cucurbituril[7] led to gating of the catalytic activity by making the catalyst inaccessible to the substrate. This was demonstrated in HeLa cells treated with the gated ruthenium containing nanoparticles. Addition of alloc-R110 only showed background signal, whereas bright fluorescence was observed upon subsequent treatment with 1-

Entry	(Pre-)catalyst	Reaction	Compartment	Cell type/ organism	Ref.
<b>Table 1. Table 1</b> Overview of intracellular transition metal-promoted reactions.					
<b>Ruthenium catalysts</b>					
1				HeLa	[22]
2				CEF	[23]
3			Au NP	HeLa	[24]
4				HeLa	[25]
5				HeLa, A549	[26]
6				HeLa	[27]
7				<i>P. aeruginosa</i> , BT474, MCF-7, zebrafish	[28]
8			SCNP	HeLa	[29]

Entry	(Pre-)catalyst	Reaction	Compartment	Cell type/ organism	Ref.
9	 streptavidin biotin 	 Umbelliferone	ArM	<i>E. coli</i>	[30]
10	 streptavidin biotin 	 Triiodothyronine	ArM	HEK293T	[31]
11	 albumin coumarin 	 Umbelliprenin	ArM	SW620	[32]
12	Copper catalysts 	 barstar protein → barstar protein		<i>E. coli</i>	[33]
13	 tetramethyl rhodamine	 paclitaxel → paclitaxel tetramethyl rhodamine		HuH-7	[34]
14		 Antimicrobial	SCNP	NCI-H460, MDA-MB-231, <i>E. coli</i>	[35]
15	Cu <sup>0</sup> NP 	 Combretastatin A4 analogue	crosslinked lipoic acid NP	HeLa	[36]
16	Cu <sup>0</sup> NP 	 Combretastatin A4 analogue	MOF	MCF-7, <i>C. elegans</i>	[37]

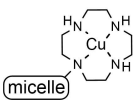
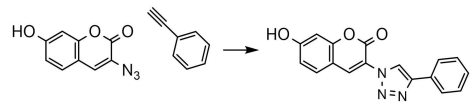
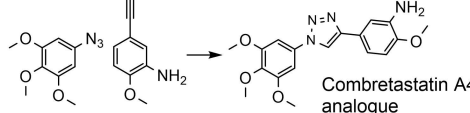
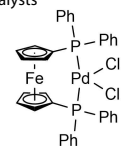
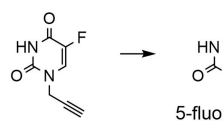
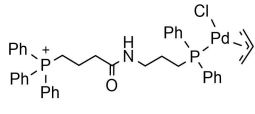
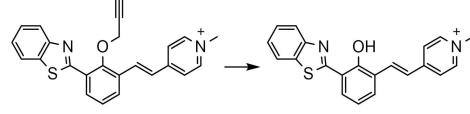
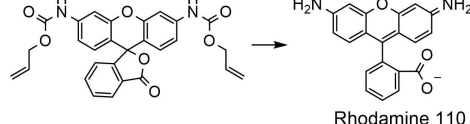
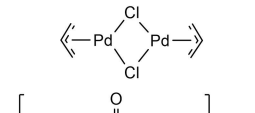
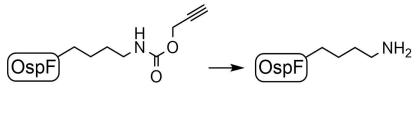
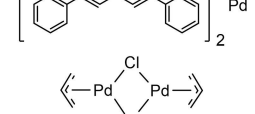
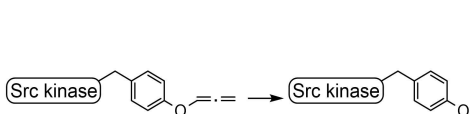
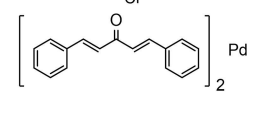
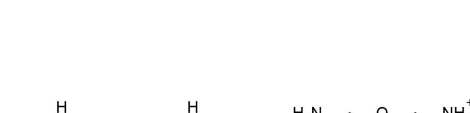
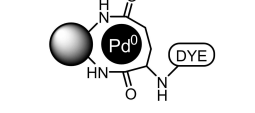
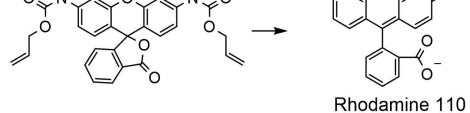
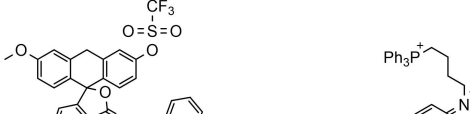
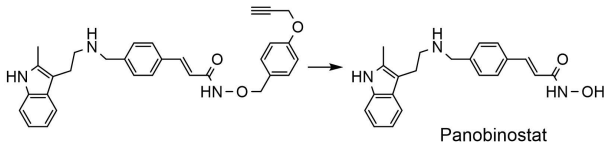
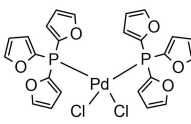
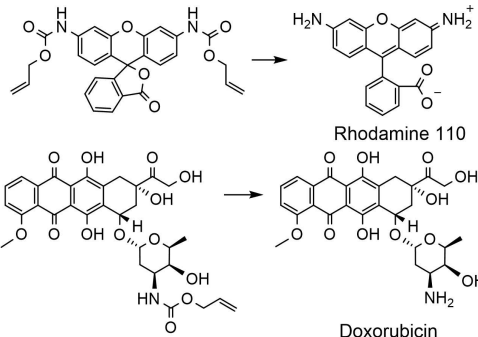
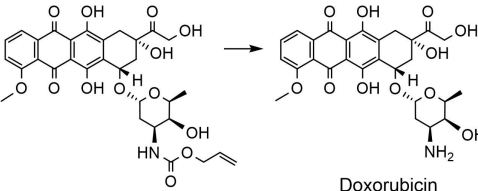
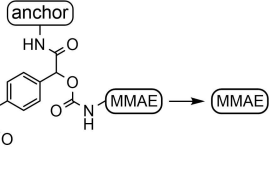
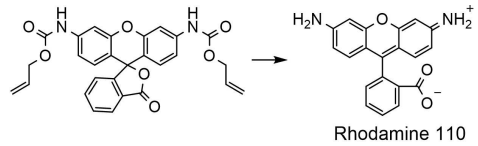

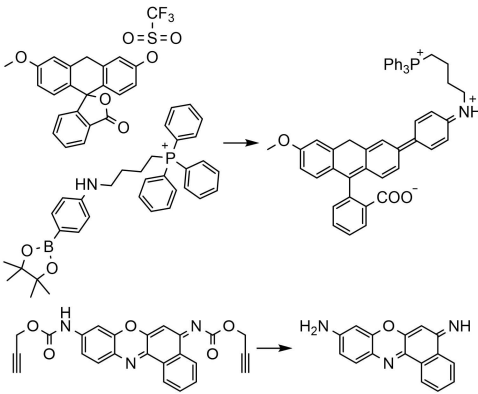

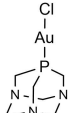
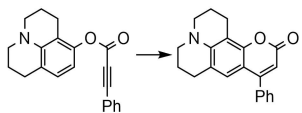
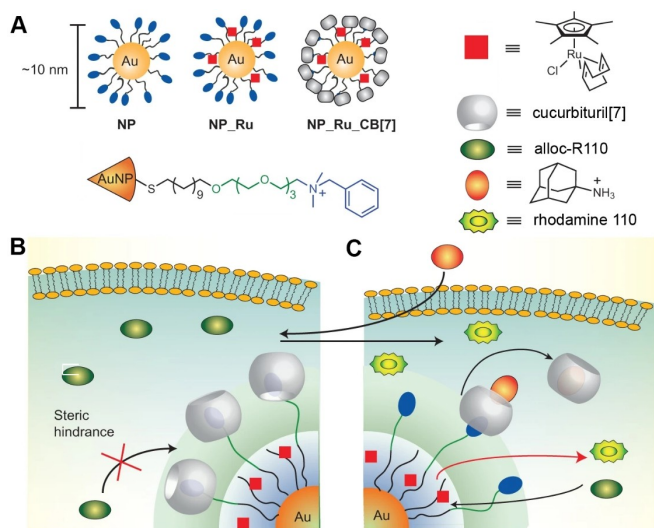
Entry	(Pre-)catalyst	Reaction	Compartment	Cell type/organism	Ref.
17	 micelle	  Combretastatin A4 analogue	Micelle	HeLa	[38]
18	Palladium catalysts 	 5-fluorouracil	Au NP	HeLa	[24]
19		  Rhodamine 110	Vero, HeLa		[39]
20		 OspF		HeLa	[40]
21		 Src kinase		HEK293T	[41]
22		 Rhodamine 110	Poly-styrene NP	HeLa	[42]
23	 peptide	  Anticancer agent PP-121		Poly-styrene NP	U87-MG [43]

Table 1. continued					
Entry	(Pre-)catalyst	Reaction	Compartment	Cell type/organism	Ref.
24	Pd <sup>0</sup> nanosheet	 Panobinostat	Exosome	A549	[44]
25		 Rhodamine 110  Doxorubicin  MMAE	PLGA- <i>b</i> -PEG micelle	HT1080, mice	[45, 46]
26	Pd <sup>0</sup> NP	 Rhodamine 110	Macro-porous silica NP	HeLa	[47]
27	 Pd <sup>0</sup> NP	 Cresyl violet	MOF	HeLa	[48]
28	 Gold catalyst 			HeLa	[27]

adamantylamine, a competitive binding agent of cucurbituril[7] (Table 1, entry 3). These nanoparticles were also successfully applied in HeLa cells in a prodrug strategy for the *in situ* activation of alloc-caged doxorubicin and the (propargyl protected) chemotherapeutic agent 5-fluorouracil (5-FU) (Table 1, entry 3, 18).<sup>[24,54]</sup>

[Ru(bpy)<sub>3</sub>]<sup>2+</sup> can facilitate azide reduction under reducing conditions upon light irradiation.<sup>[55]</sup> To demonstrate this, a fluorogenic probe was designed based on a rhodamine derivative which was caged with an azidobenzoyloxycarbonyl moiety. The reaction is not efficient in highly diluted conditions, therefore catalyst and probe were functionalized with ligands





**Figure 2.** Schematic overview of the intracellular activation of catalyst-embedded gated Au nanoparticles. A) Coated gold nanoparticles are loaded with  $[\text{Cp}^*\text{Ru}(\text{cod})\text{Cl}]$  and subsequently gated with cucurbituril[7]. B) After cellular internalization, catalytic activity is blocked by steric hindrance from cucurbituril[7]. C) Upon addition of 1-adamantylamine (red sphere), which competes for the gating cucurbituril[7], catalytic activity is restored and alloc-R110 is converted to rhodamine. Figure adapted with permission from Ref. [24]. Copyright: 2015, Springer Nature.

to achieve intracellular complexation with template proteins to bring them in proximity.<sup>[28]</sup> This led to fluorescence upon Ru-assisted photoreduction (Table 1, entry 7). This approach was also applied in miRNA imaging in cell cultures<sup>[56]</sup> and in zebrafish.<sup>[57]</sup> The same complex was integrated in a positively charged cross-linked single chain nanoparticle (SCNP).<sup>[29]</sup> Within these particles, azidified rhodamine 110 was efficiently converted in buffer and in HeLa cells, likely because of hydrophobic

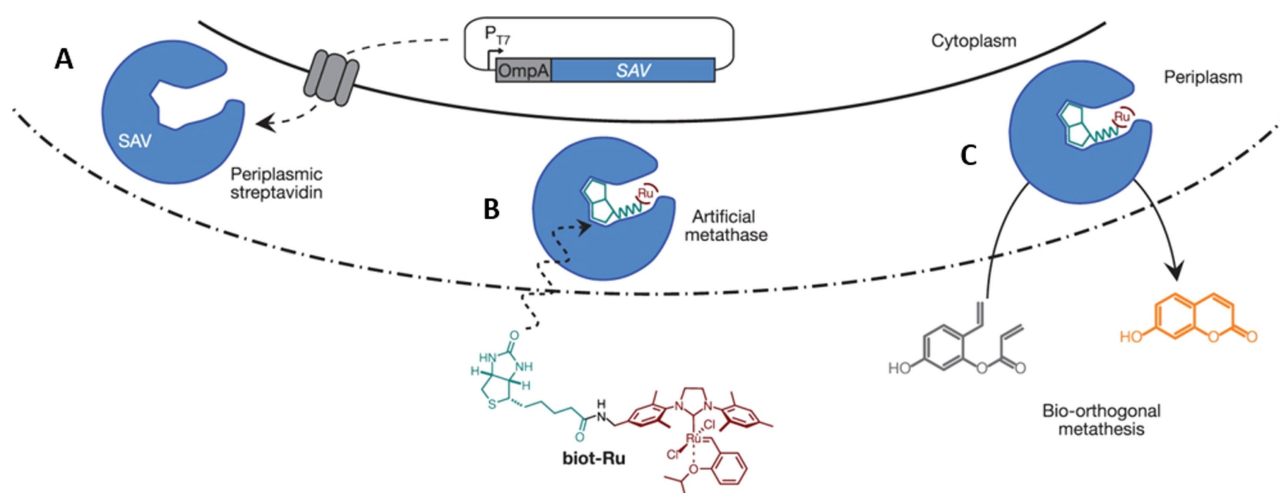
interactions which increase the local concentration of probe in the particles (Table 1, entry 8).

Intracellular tandem catalysis was then achieved by the introduction of  $\beta$ -galactosidase, which was simultaneously internalized by cells due to electrostatic interactions between the negatively charged enzyme and the SCNP. The probe consisted of an azidobenzylcarbonate-protected 4-methylumbelliferyl- $\beta$ -D-galactopyranoside, which generated fluorescence upon intracellular light-assisted conversion by the Ru-complex containing SCNP, followed by enzymatic cleavage of the sugar.

As mentioned earlier, enzymes often contain metal cofactors which are required for their catalytic activity. With this in mind, researchers have begun to explore the opportunity to artificially introduce metals to proteins to create so-called artificial metalloenzymes (ArMs).<sup>[58]</sup> Benefiting from the innate biocompatibility of proteins, a number of examples have been successfully applied in an intracellular fashion.

As a first example, streptavidin was employed by Ward et al. as proteinaceous carrier of the Hoveyda Grubbs second-generation catalyst (HGII) to allow *in cellulo* ring closing metathesis of a dye precursor (Figure 3 and Table 1, entry 9).<sup>[30]</sup> HGII was coupled to biotin to be locked inside the protein. Screening experiments showed that physiological concentrations of GSH completely inhibited the catalytic activity. Therefore, a strategy was developed to minimize catalyst poisoning by directing the ArM to the periplasmic space of *Escherichia coli*, where the GSH concentration is considerably lower than in the cytosol. To this end, streptavidin was expressed containing a periplasmic targeting sequence. Subsequently, biotin-HGII was added to the cells, followed by the substrate to yield fluorescent umbelliferone. Directed evolution was then used to enhance the activity of the ArM.

In a similar fashion, a derivative of dimethylamino-tailored  $[\text{Cp}^*\text{Ru}(\text{QA})(\text{allyl})]^+$ , developed by Meggers and co-workers, was



**Figure 3.** Schematic overview of artificial metalloenzyme-promoted metathesis in *E. coli*. A) Streptavidin (SAV) is directed to the periplasm by fusion with an OmpA translocation signal. B) Binding of biotinylated HGII catalyst to the periplasmic streptavidin leads to the formation of an artificial metathase. C) Conversion of umbelliferone precursor catalyzed by HGII-loaded artificial metalloenzyme in the periplasm of *E. coli*. Figure adapted with permission from Ref. [30]. Copyright: 2016, Springer Nature.

immobilized in streptavidin to create an alloc-cleaving ArM.<sup>[31]</sup> To achieve cellular uptake of the protein complex, the tetrameric nature of streptavidin was used. Besides complexation with the biotinylated catalyst, the structure was charged with a biotinylated poly(disulfide) cell-penetrating peptide (CPP). The tetrameric complex was able to enter HEK293T cells, which were engineered with a gene switch system for secreted nanoluciferase expression, which is repressed in absence of thyroid hormone triiodothyronine ( $T_3$ ). The ArM could uncage alloc-protected  $T_3$ , resulting in an increase in luminescence (Table 1, entry 10). This catalytic activity was demonstrated to be higher than when free (non-biotinylated) Ru-complex was used.

The viability of ArMs has also been examined in a prodrug strategy.<sup>[32]</sup> For cellular uptake, the protein was functionalized with  $\alpha(2,3)$ -linked sialic acid terminated *N*-glycans, which were previously shown to target certain cancer cells. As prodrug, a precursor of the anticancer agent umbelliprenin was used, which is converted into the active compound upon ring closing metathesis (Table 1, entry 11). Incubation of cancer cells with the glycosylated ArM together with the prodrug significantly decreased cell proliferation to below 5%, whereas non-glycosylated ArM was considerably less effective. It must be noted, however, that it is unclear whether the ArMs accumulate on the cell surface or are active intracellularly.

## 2.2. Copper-mediated intracellular catalysis

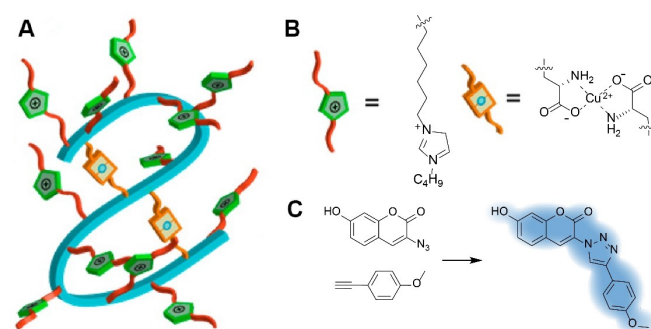
Copper is an obvious candidate as transition metal for intracellular catalysis, as it is an endogenous component of cells. An excess of copper is toxic to cells, therefore its presence is strictly regulated by copper-binding chaperones and transporters.<sup>[59]</sup> Copper toxicity is mainly attributed to the ability of  $Cu^I$  to catalyze the production of reactive oxygen species. A catalytic conversion which has shown good biocompatibility and application potential in intracellular organometallic-based catalysis is the copper-catalyzed azide-alkyne cycloaddition (CuAAC).<sup>[60,61]</sup> Biocompatibility of this reaction was, to some extent, already shown by its successful execution in the soluble fraction of cell lysate.<sup>[62]</sup> The first example employing living cells demonstrated efficient labeling of proteins on the cell surface of *E. coli* using CuAAC.<sup>[63,64]</sup> Notably, the cells could not divide anymore in rich medium after the copper catalyzed labeling had taken place. The first example of CuAAC inside live cells involved auxotrophic *E. coli* bacteria which were supplied with alkyne-containing unnatural amino acids 4-ethynylphenylalanine or homopropargylalanine incorporated in the barstar protein.<sup>[33]</sup> Treatment with  $CuBr$  or  $CuSO_4/TCEP$ , together with the ligand tris (benzyltriazolylmethyl)amine (TBTA) and 3-azido-7-hydroxycoumarin led to Cu-catalyzed intracellular protein labeling (Table 1, entry 12).

The translation to using CuAAC in the interior of living mammalian cells proved to be more cumbersome, likely due to toxicity of  $Cu^I$  and sodium ascorbate (NaAsc), even in the presence of TBTA.<sup>[65]</sup> Furthermore, the reaction exhibited slow

kinetics.<sup>[66]</sup> CuAAC with TBTA could only effectively be performed on fixed cells,<sup>[67-71]</sup> with the exception of surface glycan labeling of living *Saccharomyces cerevisiae*.<sup>[72]</sup> With the application of tris(3-hydroxypropyltriazolylmethyl)amine (THPTA),<sup>[73]</sup> and a range of more water-soluble ligands, cellular toxicity was significantly decreased,<sup>[74-76]</sup> and labeling of cell surface glycans and proteins of living mammalian cells and zebrafish embryos was accomplished.<sup>[74-81]</sup> The performance of CuAAC was further improved by employing azides with an additional copper-chelating moiety.<sup>[82]</sup> This was applied in a biological setting for labeling live HEK cell membrane proteins using picolyl azides and also for labeling RNA and proteins inside fixed cells.<sup>[81]</sup> Inspired by this work, the first intracellular CuAAC in live mammalian cells was reported. Taran and co-workers prepared azide substrates tailored with different bis (triazolylmethyl)amine moieties for chelation-assisted copper catalysis (Table 1, entry 13).<sup>[34]</sup> Screening assays in aqueous medium showed CuAAC yields up to 75% within a few minutes. In this manner, tubulin-targeting paclitaxel was labeled with a dye inside HuH-7 cells. The disadvantage of this system is that the catalyst is likely sequestered by the product.

Nanoformulations could be a solution to the adverse effects of the intracellular environment to the catalyst and vice versa. For this purpose a copper-nanoparticle formulation was prepared using highly positively charged SCNPs with aspartate moieties and quaternized imidazoles, which were physically crosslinked by  $Cu^{II}$  (Figure 4A, B).<sup>[35]</sup> Together with a high concentration of NaAsc (2 mM), they were shown to catalyze intracellular CuAAC between 3-azido-7-hydroxycoumarin and 4-ethynylanisole in NCI-H460 and MDA-MB-231 cells (Figure 4C and Table 1, entry 14). Additionally, an antimicrobial agent was synthesized in *E. coli* in this manner. The SCNPs were highly effective as CuAAC was achieved with low copper concentrations, however the high concentration of NaAsc, as well as the non-biodegradable nature of the polymer are disadvantageous for applications in living systems.

The effect of the shape of a nanocarrier on the intracellular activity of the catalyst was shown by Zhang et al.<sup>[36]</sup> Nanoparticles were prepared by reducing lipolic acid above its critical



**Figure 4.** Schematic overview of a catalytic single-chain nanoparticle. A) Positively charged single chain nanoparticle crosslinked by complexation with  $Cu^{II}$ . B) Schematic representation of quaternized imidazole moiety and  $Cu^{II}$ -aspartate crosslinking complex. C) CuAAC reaction scheme of the generation of a fluorescent coumarin derivative. Figure adapted with permission from Ref. [35]. Copyright: 2016, American Chemical Society.

aggregation concentration with dithiothreitol. Subsequent copper(0) encapsulation was achieved using  $\text{CuSO}_4$  and  $\text{NaBH}_4$  to give rugby-ball-shaped nanoparticles. These could be turned into small spherical nanoparticles of approximately 11 nm by an additional  $\text{NaBH}_4$  treatment. Exposure to UV light gave spherical particles of approximately 47 nm. The rugby-ball-shaped particles were best taken up by HeLa cells and generated the highest fluorescent response after the cells were incubated with 3-azido-7-hydroxycoumarin and phenylacetylene (Table 1, entry 15). The catalysts were then used for intracellular synthesis of an analogue of cytotoxic tubulin polymerization inhibitor Combretastatin A4, a strategy used before when SKOV-3 cells were treated with Cu-loaded nanoparticles.<sup>[83]</sup>

Another strategy to achieve intracellular CuAAC involved 120 nm sized metal-organic frameworks (MOFs) prepared from  $\text{ZrCl}_4$  and aminoterephthalic acid decorated with copper(0) nanoparticles.<sup>[37]</sup> Additionally, they were tailored with triphenylphosphonium moieties for mitochondrial targeting. Intracellular activity was first shown using the 3-azido-7-hydroxycoumarin probe (Table 1, entry 16). Then a resveratrol analogue was synthesized intracellularly which created mitochondrial damage as shown by cell viability assays, reactive oxygen species (ROS) detection and indications of apoptosis. When resveratrol was given directly to cells, this effect was not observed, meaning that localized synthesis had a large effect on the mitochondria. *C. elegans* were fed with the copper-MOFs and lit up blue after incubation with 3-azido-7-hydroxycoumarin and phenylacetylene, showing the biocompatibility of the catalyst.

Micelles represent another nano-formulation in which copper has been loaded. They were prepared from unimers consisting of diallylamine coupled to cyclen via a dodecane linker.<sup>[38]</sup> They were crosslinked by Michael addition using dithiothreitol and supplied with  $\text{Cu}^I$ , located at the surface of the particles. In HeLa cells, they were able to catalyze CuAAC between 3-azido-7-hydroxycoumarin and phenylacetylene (Table 1, entry 17).

### 2.3. Palladium-mediated intracellular catalysis

Palladium is one of the most widely used metal catalysts in organic synthesis.<sup>[84,85]</sup> Because of its broad tolerance to functional groups and applicability in aqueous solutions, it exhibits promising features as a biocompatible catalyst. To make it amenable to biological substrates, much research has been done in the development of water-soluble ligands for aqueous Pd-mediated catalysis.<sup>[86,87]</sup> These ligands have been used to functionalize nucleotide derivatives,<sup>[88]</sup> peptides<sup>[89–91]</sup> and proteins.<sup>[92–94]</sup> However, all reactions were carried out under a protective atmosphere and sometimes using elevated temperatures or co-solvents. The first efficient biocompatible procedure was reported in 2009, when a protein tailored with a chemically introduced 4-iodophenyl moiety was coupled to a variety of boronic acids via Suzuki-Miyaura cross-coupling in excellent yields.<sup>[95]</sup> For this reaction a large excess of a combination of  $\text{Pd}(\text{OAc})_2$  and 2-amino-4,6-dihydropyrimidine (ADHP) was used.<sup>[96]</sup> In a different approach, 4-iodophenylala-

nine was genetically incorporated in a protein and subjected to Suzuki-Miyaura coupling using the same catalyst-ligand combination.<sup>[97]</sup> This strategy was successfully employed to label membrane protein OmpC on the surface of live *E. coli* cells with boronic acid-tailored fluorophores<sup>[98]</sup> and sugars.<sup>[99]</sup> Although ligand optimization resulted in better catalytic activity, still high amounts of catalyst and reagent were required for coupling to proteins.<sup>[100]</sup> Cell-surface labeling of mammalian cells was also achieved.<sup>[101]</sup> HeLa cells were first functionalized with aryl iodide groups using *N*-succinimidyl-*p*-iodobenzoate. This was followed by Suzuki-Miyaura coupling with arylboronic acid-tailored biotin.

A study by Mascareñas et al. demonstrates the importance of choosing the right ligands for a catalyst complex in living systems.<sup>[39]</sup> Several palladium complexes were examined for their ability to catalyze depropargylations and alloc cleavages in aqueous media. Water-soluble complexes with pyridine or methionine-based ligands were the best candidates in simple aqueous media, whereas more hydrophobic phosphine-tethered complexes acted poorly. In cell lysates, the inverse was true. The water-soluble complexes were not stable enough to survive the hostile environment, whereas the phosphine-containing complexes were able to convert the substrate. These catalysts were able to depropargylate probes and cleave alloc groups in Vero and in HeLa cells (Table 1, entry 19). It must be noted that the cells were incubated with probe before the catalyst was introduced to the cells. In case of the depropargylations, no significant fluorescence was observed when the inverse protocol was followed.

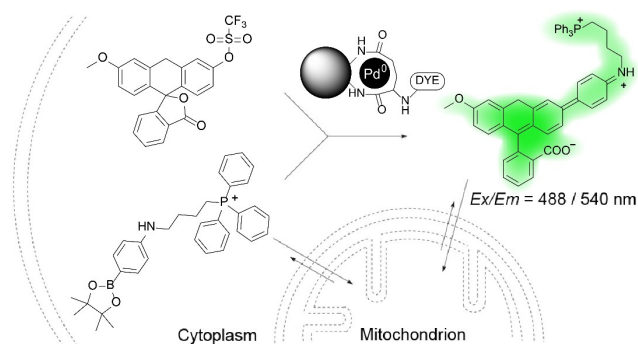
Palladium-species  $\text{Pd}(\text{dba})_2$  and  $\text{Pd}_2\text{allyl}_2\text{Cl}_2$  were demonstrated to reactivate proteins in living cells.<sup>[40]</sup> To this end, OspF was expressed in HeLa cells, containing a lysine protected with a propargyloxycarbonyl (poc) group in its active site. The poc group was chosen over the alloc group, because it was shown to be cleaved more efficiently in PBS. This was also observed in a previous study.<sup>[102]</sup> OspF can irreversibly dephosphorylate ERK kinase via an elimination route to give a trisubstituted alkene instead of the phosphorylated threonine. Using immunoassays, it was shown that poc-containing OspF could not dephosphorylate ERK in HeLa cells. This activity was restored to some extent by loading the cells with either of the two Pd catalysts (Table 1, entry 20).

An additional protein gain of function study involved allene-caged tyrosine residues.<sup>[41]</sup> The activity of a Src kinase mutant containing an allene-caged tyrosine could be restored intracellularly upon incubation with either  $\text{Pd}_2\text{allyl}_2\text{Cl}_2$  or  $\text{Pd}(\text{dba})_2$  (Table 1, entry 21).

A range of different carrier systems have been reported to facilitate palladium-mediated catalysis in living cells. Bradley et al. loaded amine-presenting polystyrene nanoparticles with  $\text{Pd}(\text{OAc})_2$  and reduced this to  $\text{Pd}^0$  using hydrazine.<sup>[42]</sup> The spheres were taken up by cells to convert alloc-R110 (Table 1, entry 22). Furthermore, they demonstrated the ability of the Pd spheres to promote an intracellular C–C bond formation reaction via Suzuki-Miyaura coupling of a triflate-containing fluorescein-like profluorophore and an alkylaminophenylboronic acid pinacol ester tagged with a mitochondria-targeting

moiety (Figure 5). Imaging on fixed cells showed mitochondrial localization of the product. Pd<sup>0</sup> resins were hereafter used for the uncaging or *in situ* synthesis of several prodrugs in mammalian cell culture.<sup>[103]</sup> To further improve on selective particle uptake the Pd-nanoparticles were functionalized with cRGDfE peptides, which have affinity for cells expressing the  $\alpha_v\beta_3$  receptor, such as U87-MG cells.<sup>[43]</sup> The nanoparticles were shown to create intracellularly the cytotoxic PP-121 via Suzuki-Miyaura coupling, leading to decreased cell viability (Table 1, entry 23). Pd<sup>II</sup> has been introduced to cells using a similar peptide, HRGDH, where it was catalytically active.<sup>[104]</sup>

Recently, a new strategy was applied to introduce palladium nanoparticles to cells, involving exosomes.<sup>[44]</sup> Such vesicles bud from their progenitor cells for communication purposes and preferentially reach cells of the same cell type. Although it is difficult to isolate them and keep them stable over time, they are promising vectors for targeted delivery. A549 exosomes were incubated with water-soluble K<sub>2</sub>PdCl<sub>4</sub>, purified and exposed to 6 bars of CO gas to create palladium(0) nanosheets

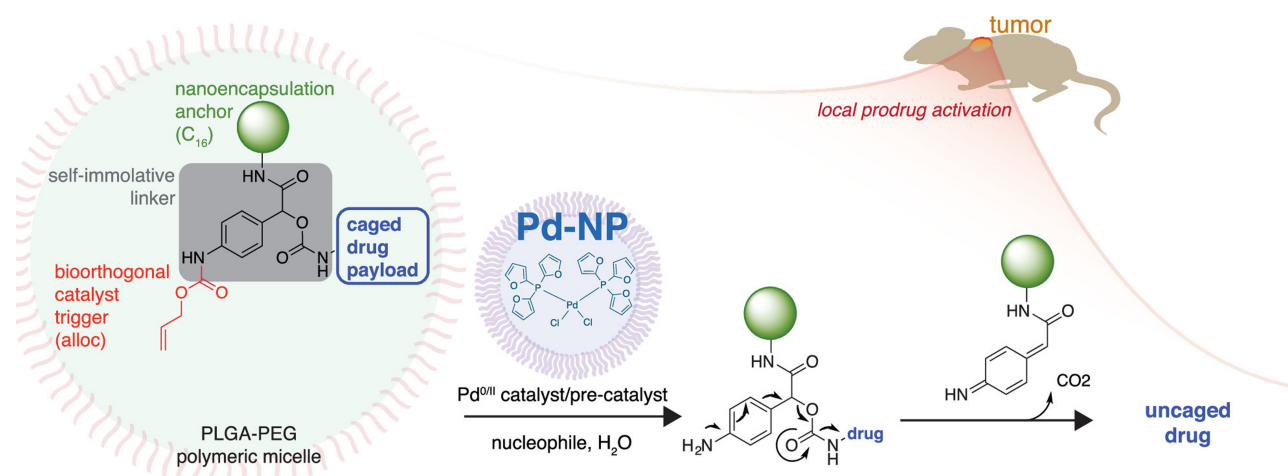


**Figure 5.** Schematic overview of intracellular Suzuki-Miyaura coupling promoted by Pd<sup>0</sup>-loaded polystyrene nanoparticles. A fluorescent mitochondrial tracker is prepared upon coupling of a profluorophore to a triphenylphosphonium moiety. Figure adapted with permission from Ref. [42]. Copyright: 2011, Springer Nature.

within the exosomes. CO was the reductant of choice, since it is relatively mild to minimize damage to exosomal proteins. The Pd-exosomes were used for prodrug activation. Anti-tumor drug panobinostat was modified with a self-immolative linker, conjugated to a propargyl ether to enable Pd-mediated uncaging (Table 1, entry 24). Due to the cell-specific uptake of the exosomes, the cell viability of A549 cells significantly decreased, whereas this was not observed for U87 cells.

Pd-nanoparticle promoted alloc-cleavage reactions were investigated by Weissleder et al. in a biomedical context.<sup>[45]</sup> Highly lipophilic PdCl<sub>2</sub>(TFP)<sub>2</sub> was encapsulated in poly(lactic-co-glycolic acid)-poly(ethylene glycol) (PLGA-PEG) micelles. In this manner, better bioavailability and protection of the catalyst against the environment was achieved, as well as accumulation in tumors because of the enhanced permeability and retention effect.<sup>[105]</sup> Also, cellular uptake using the Pd-nanoparticles was higher compared to incubation with the free Pd complex. The catalytic activity was examined in HT1080 cell cultures, which were treated with the Pd-loaded nanoparticles (NPs) and with either alloc-R110 or a procoumarin substrate for Heck reactions. After washing, both cell cultures showed a fluorescent signal. However, it was not clear whether the cleavage and Heck reaction mainly occurred in the medium or intracellularly or both. Finally, the Pd-nanoparticles were shown to accumulate in tumor tissue in live mice and activate alloc-protected doxorubicin (Table 1, entry 25).

A further improvement was made by immobilizing the prodrug into separate PLGA-PEG micelles via a self-immolative linker and a Pd-cleavable group (Figure 6).<sup>[46]</sup> In this dual nanotherapy strategy, the EPR effect was used to increase the local tumor concentration of catalyst and prodrug, with minimal leakage of the prodrug. The PLGA-PEG micelles were shown to end up in late endosomes and lysosomes of HT1080 cells. Co-localization of pro-doxorubicin anchored micelles and Pd-NPs was demonstrated, followed by accumulation of doxorubicin in the nucleus, suggesting that the catalysts were intracellularly active. Another prodrug, caged monomethyl auristatin E



**Figure 6.** Schematic overview of Pd-mediated activation of a compartmentalized prodrug in mice. The caged prodrug and PdCl<sub>2</sub>(TFP)<sub>2</sub> are loaded into separate PLGA-PEG micelles, which are then injected into mice. There, the drug is released by Pd-catalyzed alloc cleavage and subsequent degradation of the self-immolative linker. Figure reproduced with permission from Ref. [46]. Copyright: 2018, Miller et al.

(MMAE), was also anchored in micelles. When cells were co-incubated with the catalyst and the prodrug particles,  $IC_{50}$  values were achieved of almost those of native MMAE (Table 1, entry 25).

Photo-activatable palladium nanoparticles have also been developed.<sup>[47]</sup> Nanopalladium loaded macroporous silica nanoparticles were functionalized with azobenzene moieties and subsequently closed with cyclodextrin via host-guest interactions to block the entrances to the catalyst. Cyclodextrin was released upon light irradiation, due to azobenzene isomerization, clearing the way for substrates. In this manner, allocleavage and Suzuki-Miyaura coupling was achieved in HeLa cells (Table 1, entry 26).

Recently, Pd nanocubes were encapsulated inside polymer-stabilized Zn-based zeolitic imidazolate frameworks (ZIF-8) as a means to provide protection of the catalyst against external stimuli.<sup>[48]</sup> The Pd-MOFs were catalytically active inside cells, demonstrated by uncaging of poc-protected cresyl violet (Table 1, entry 27). When the cells were washed and exposed to fresh substrate, a rise in fluorescence was observed again. This was repeated up to 4 cycles, proving that the particles remained active over a longer time. In contrast to several discrete Pd complexes as well as non-encapsulated Pd NPs, which were less active and did not show activity during the second cycle.

## 2.4. Gold-mediated intracellular catalysis

Cationic gold species are so called carbophilic catalysts, they selectively activate acetylenes to make them susceptible to nucleophilic attack.<sup>[106–108]</sup> Furthermore, they are relatively stable towards oxygen and moisture. These properties make them suitable biocompatible catalysts.

The two first cases of *in vivo* gold-promoted catalysis do not specifically target the intracellular environment. In one example, a coumarin-tailored  $Au^{III}$  catalyst was complexed with albumin.<sup>[109]</sup> The type of protein-surface glycosylation determined the fate of the catalyst. In this manner, the liver and intestines were labeled in a targeted fashion by propargyl ester probes. In the other example, a heterogenous catalyst was prepared by growing nanometer sized gold beads onto a 75 micron-sized solid support.<sup>[110]</sup> This was surgically placed in the brain of zebrafish larvae and showed local conversion of poc-caged R110.

Recently, gold nanorods have been introduced to cells together with  $TiO_2$  NPs inside a silica shell for localized photodegradation of rhodamine B and generation of ROS.<sup>[111]</sup> In another intracellular approach, a gold-complex was shown to be catalytically active inside cells.<sup>[27]</sup> Several Au–Cl complexes were screened for their reactivity as well as their toxicity to cells. As most complexes showed good to excellent activity in water, considerable differences in cytotoxicity were observed, depending on the coordinating ligand. The most suitable complex was examined in a variety of media, resulting in the observation that GSH and cysteine completely abolished catalytic activity. Nevertheless, it was possible to convert a

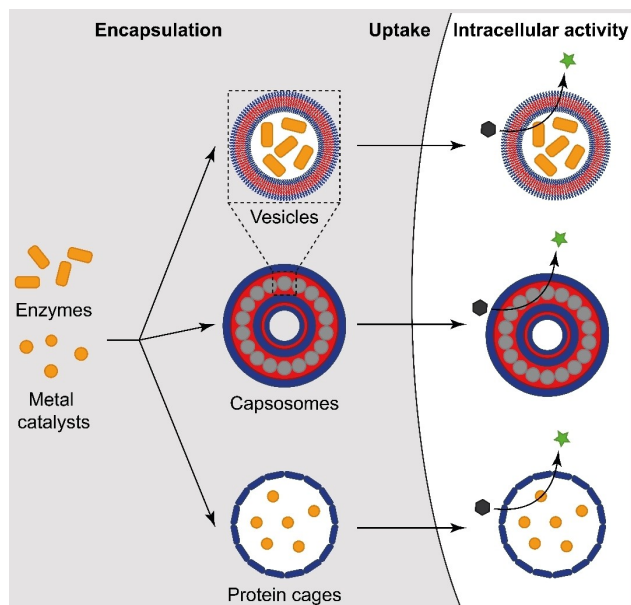
coumarin dye precursor inside living cells via hydroarylation (Table 1, entry 28). The reaction was also carried out in living cells in the presence of another catalyst. A phosphonium tagged Ru catalyst was chosen to deallylate a profluorescent compound to give an infrared emitter (Table 1, entry 6). Cells that were treated with both catalysts, followed by the probes, showed fluorescence of both products.

## 3. Premade Semisynthetic artificial organelles

Although organometallic complexes often have the ability to cross the cell membrane because of their hydrophobic nature, cellular uptake of other catalysts, such as free enzymes is very limited. A carrier is therefore essential to transport an externally produced enzyme over the cell membrane. Furthermore, free enzymes are susceptible to proteolytic degradation and direct functionalization to improve stability or cellular uptake often comes at the cost of catalytic activity. Encapsulation inside a micro- or nanovehicle offers two main advantages. It offers protection against external stimuli and secondly, the carrier can be functionalized in order to facilitate cellular internalization or target a specific cell type without affecting the enzyme in its interior. Such a compartment needs to meet certain requirements. Low immunogenicity and toxicity are essential. The structure is preferably bio-degradable, so it can be eventually cleared from the cell to avoid accumulation of abiotic material. Moreover, the compartment needs to allow a flux of substrate and product to allow the catalytic entity to carry out its function and to prevent a local build-up of product. This is generally achieved either via the installation of pore proteins or by using a membrane which is inherently semi-permeable and thereby allows for the diffusion of small molecules. As such, the biggest developments have been made with polymer-based and protein-based nanoreactors (Figure 7). As both of these systems have been extensively reviewed,<sup>[112–114]</sup> they will only be discussed here in brief.

### 3.1. Polymer-based nanoreactors

Architectures of different nature have been applied as artificial organelles, ranging in material, composition and size.<sup>[115]</sup> Of these, polymersomes are the most represented. These are polymeric nanometer-range sized vesicular assemblies which are able to encapsulate compounds in their aqueous lumen. Polymersomes prepared from triblock co-polymer poly(methyloxazoline)-poly(dimethylsiloxane)-poly(methyl-oxazoline) (PMOXA-*b*-PDMS-*b*-PMOXA) containing different (bio) catalysts, for example, trypsin,<sup>[116]</sup> Super oxide dismutase (SOD) together with lactoperoxidase,<sup>[117,118]</sup> horseradish peroxidase (HRP)<sup>[119]</sup> and a  $Cu^{II}$  complex with anti-oxidant properties,<sup>[120]</sup> have been demonstrated to act as intracellular organelles. Superoxide and highly hydrophobic compounds were able to spontaneously diffuse across the membrane, but to grant access to bigger hydrophilic molecules, protein pore OmpF was installed in the membrane. By modifying this protein, a



**Figure 7.** Schematic representation of strategies leading towards the *in vitro* production of semisynthetic artificial organelles. Enzymes can be encapsulated in vesicles, which consist of either amphiphilic polymers (polymerosomes), lipids (liposomes) or a combination of poly-anioners and cationers (PICsomes). Alternatively, enzymes can be encapsulated in multicompartmentalized carriers, capsosomes, consisting of enzyme-loaded lipid vesicles that are embedded in a polyelectrolyte layer by layer capsule. Another encapsulation strategy is to load protein cages with enzymes or metal catalysts. After cellular uptake, these semisynthetic artificial organelles demonstrate transient intracellular activity.

stimulus-responsive artificial organelle was produced. An OmpF mutant with surface cysteines was capped with a fluorophore through a disulfide bond to block the entrance of the porin protein.<sup>[119]</sup> It was envisioned that the presence of endogenous thiols, such as GSH, would release the cap through disulfide exchange to make the interior of the polymerosome accessible to substrates. As catalytic species, HRP was encapsulated which can convert Amplex Ultra Red into a fluorescent product in the presence of  $H_2O_2$ . *In vitro* assays showed a 36% reduced turnover compared with noncapped nanoreactors. After cellular uptake in HeLa cells, the capped as well as the non-capped polymerosomes caused the cells to light up when incubated with the probe and  $H_2O_2$ . The nanoreactors were shown to be biocompatible in zebrafish embryos. The vesicles co-localized with macrophages, in which they converted the probe using endogenous  $H_2O_2$ .

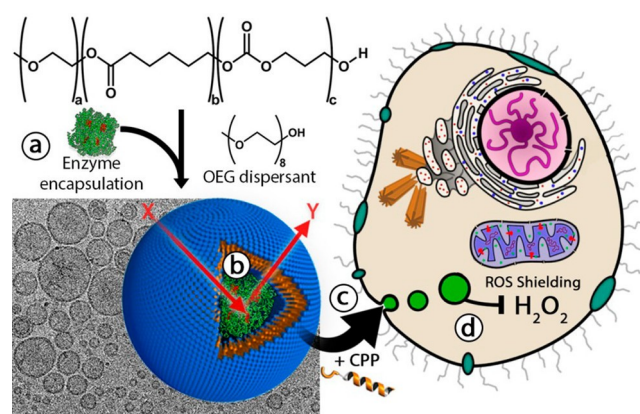
To improve cellular uptake, intrinsically semipermeable polymerosomes loaded with HRP were assembled out of polystyrene-*b*-poly(isocyno-alanine(2-thiophen-3-yl-ethyl) amide) (PS-PIAT) and polystyrene-*b*-poly(ethylene glycol) (PS-PEG) functionalized with CPP Tat.<sup>[121]</sup> Still 42% of the initial intracellular activity of HRP was present after 16 hours. Instead of mixing different synthetic polymers, lipids and block copolymers have been combined to make hybrid nanoreactor vesicles.<sup>[122]</sup> They were composed of poly(cholesteryl methacrylate)-block-poly(2-(dimethylamino) ethyl methacrylate) (pCMA-*b*-pDMAEMA) and 1-palmitoyl-2-oleoyl-sn-

glycero-3-phosphocholine and loaded with glucose oxidase (GOx) or  $\beta$ -galactosidase. Catalytic activity was demonstrated inside 264.7 RAW macrophages, where GOx elevated ROS levels and  $\beta$ -galactosidase created nitric oxide from  $\beta$ -gal-NONOate. The same block co-polymer was used to prepare micelles containing a manganese complex with anti-oxidant properties. The structures protected HepG2 cells against oxidative stress.<sup>[123]</sup> This specific cationic block co-polymer was chosen for its ability to induce endosomal/lysosomal escape through the proton sponge effect. This leads to a rupture of the endogenous vesicles, resulting in release of the entire endosome/lysosome into the cytosol, which affects cell viability.

To fulfill the requirement of biodegradability of the carrier, polymerosomes prepared from poly(ethylene glycol)-*b*-poly( $\epsilon$ -caprolactone-*g*-trimethylene carbonate) (PEG-*b*-P(CL-*g*-TMC)) were designed (Figure 8).<sup>[124]</sup> During self-assembly in a mixture of water and non-toxic oligo(ethylene glycol), they were loaded with catalase. Functionalization with Tat was shown to boost cellular internalization in mitochondrial complex-I-deficient primary fibroblasts. There, the artificial organelles offered protection against exogenous  $H_2O_2$  showing the therapeutic potential of such nanoreactors.

The *in vivo* potential of nanoreactors was shown in a prodrug approach for cancer therapy. The enzyme  $\beta$ -galactosidase was encapsulated in pegylated polyion complex vesicles (PICsomes), prepared from block anioner PEG-*P*(Asp) and homocationer *P*(Asp-AP).<sup>[125]</sup> They were crosslinked using EDC to give stable semipermeable enzyme-loaded vesicles. These accumulated in the tumor of tumor-bearing mice, where a fluorogenic probe was subsequently converted. A similar strategy was used with polymerosomes to convert  $\beta$ -D-galactopyranoside caged doxorubicin into its active component. Activity was demonstrated in HeLa cells and in tumor-bearing mice.<sup>[126]</sup>

Liposomes have also been used as carrier systems to introduce functional cargo into cells. They were filled with all



**Figure 8.** Schematic overview of biodegradable artificial organelles. A) PEG-*b*-P(CL-*g*-TMC) polymerosomes were loaded with catalase. B) Inherent semi-permeability allows for a flux of substrate (x) and product (y). C) Cellular internalization is enhanced by functionalization of polymerosomes with cell-penetrating peptides. D) Catalase-mediated intracellular protection against  $H_2O_2$ . Figure reproduced with permission from Ref. [124]. Copyright: 2018, Van Oppen et al.

components of a PCR mixture and internalized by CHO-K1 cells leading to synthesis of a red fluorescent protein.<sup>[127]</sup> This indicates either escape of the DNA from the liposome, or disruption of the vesicle. In another study, GFP mRNA amplification machinery was introduced to blood platelets, which are not nucleated.<sup>[128]</sup> The onset of intracellular mRNA synthesis involved light irradiation to free caged ATP. Increased levels of mRNA were detected. However, subsequent transcription was not mentioned.

The use of multicompartiment carriers is especially appealing, because it opens the possibility of multiple confined processes to take place simultaneously within the same carrier system. Such a system, composed of  $\beta$ -lactamase-loaded liposomes within a polyelectrolyte layer by layer capsule was designed by Caruso et al.<sup>[129]</sup> The so-called capsosomes were prepared using a silica template core which was finally removed without affecting enzymatic activity. It was for the first time applied in an intracellular fashion with GOx as catalytic species.<sup>[130]</sup> In this setup, the particles were fortified with a layer of polydopamine and tailored with RGD peptides for cellular uptake. The silica core was not removed before utilization in a cellular context. RAW 264.7 macrophages which had internalized the microreactors were incubated with high concentrations of glucose, resulting in toxicity due to GOx-mediated  $H_2O_2$  formation.

Multicompartimentalized carriers can also promote reactions in parallel.<sup>[131]</sup> Capsosomes were prepared having two different liposome populations, either containing HRP or trypsin. The thiol-containing outer layer was crosslinked with bis-maleimide functionalized linkers. The resulting two-enzyme microreactor was internalized by RAW 264.7 macrophages and activity was shown by the generation of fluorescence upon incubation with Amplex Red,  $H_2O_2$  and Bis-(CBZ-Ile-Pro-Arg)-R110. Using another combination of enzymes, an intracellular cascade reaction could be carried out by the capsosomes.<sup>[132]</sup> GOx and HRP were incorporated and the vectors were internalized by RAW 264.7 macrophages. There, GOx oxidized glucose to give  $H_2O_2$  as byproduct, which could subsequently be used by HRP to convert Amplex Red into resorufin.

To complement the inner catalytic activity, capsosomes were equipped with an outer layer with non-enzymatic anti-oxidant properties.<sup>[133,134]</sup>

### 3.2. Protein-based nanoreactors

There are many protein-based cage structures that can be used for artificial organelle development. For example, due to their natural capacity to store iron, ferritins can be engineered into metal-catalyst-containing nanoreactors.<sup>[135,136]</sup> As ferritins are hollow spheres that naturally can accommodate up to 4500 iron atoms, their 8 nm inner diameter provides sufficient space to incorporate other metal ions and complexes as well. Moreover, re-engineering of key subunit interfaces has led to the development of slightly smaller<sup>[137]</sup> and larger<sup>[138]</sup> ferritin cages, indicating that the size can be tuned to accommodate a variety of cargoes optimally. As such, ferritins were used for the

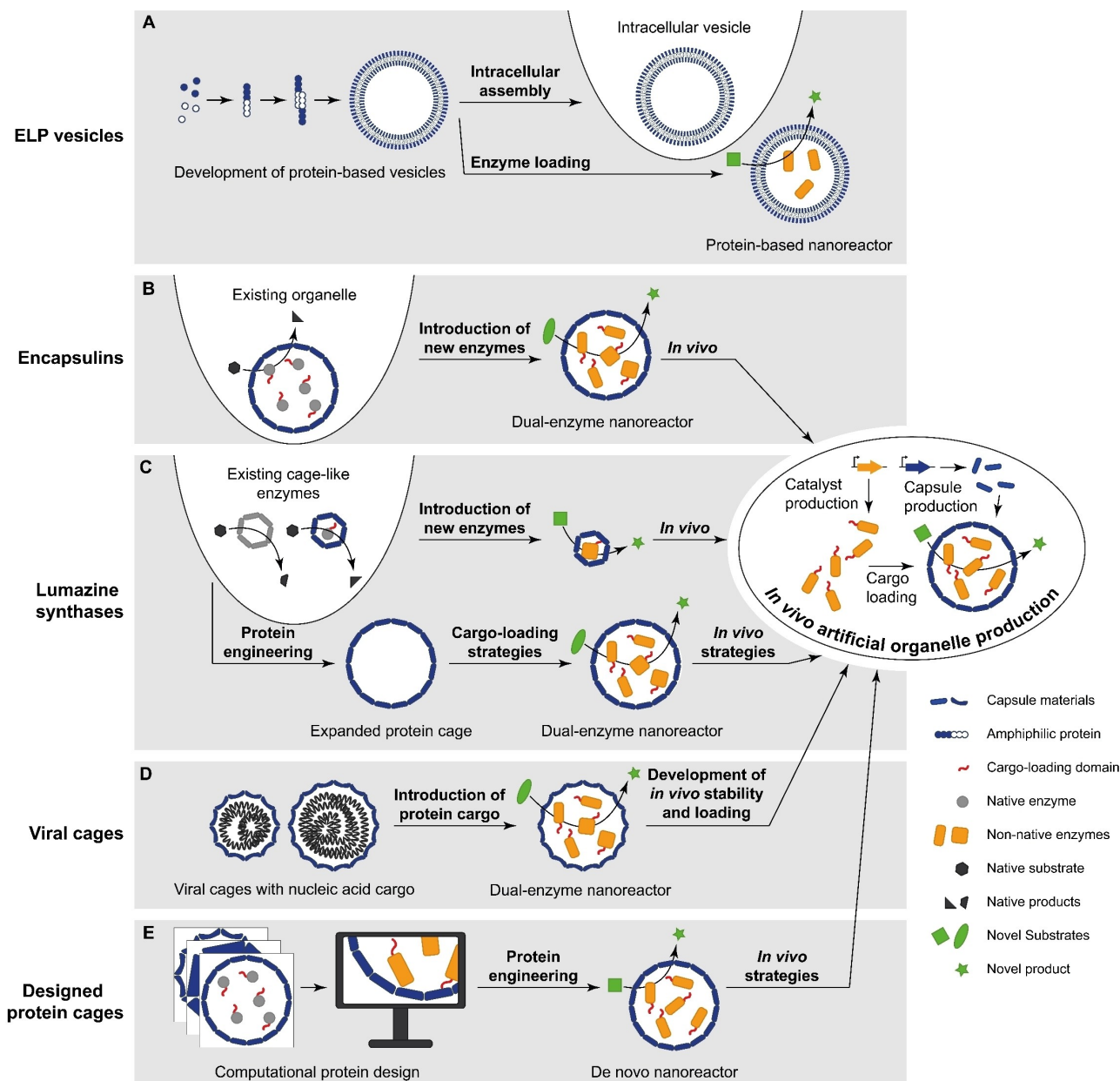
templated formation of manganese oxide from  $Mn^{II}$  and  $MnO_4^-$ ,<sup>[139]</sup> gold nanoparticles from various gold complexes,<sup>[140]</sup> and palladium nanoparticles from  $Pd^{II}$  salts,<sup>[141]</sup> of which the latter could be used *in vitro* to catalyze the oxidation of primary and secondary alcohols in aqueous solutions. More importantly, ferritins loaded with  $CeO_2$  nanoparticles were used as SOD-mimic in a live-cell system.<sup>[142]</sup> Not only was the apoferritin- $CeO_2$  complex 3.5 times more active as ROS scavenger *in vitro* than a control SOD, but encapsulation by ferritin also increased the intracellular uptake of the nano- $CeO_2$  as well as the oxidative stress relief of the cells. Besides metal catalysts, also enzymes have been encapsulated into ferritins. For example, Hilvert and co-workers developed an efficient cargo-loading strategy based on electrostatic interactions with the anionic core of the *Archaeoglobus fulgidus* ferritin by fusing positively supercharged GFP tags to various enzymes.<sup>[143]</sup> It was demonstrated that the enzymes retained high activity *in vitro* and were protected against proteolysis and heat. Via the same strategy Kostianen and co-workers have encapsulated a lysozyme inside the *Thermotoga maritima* ferritin cage.<sup>[144]</sup> Most interestingly, this enzyme encapsulation method was reversible *in vitro* under mild conditions and in addition the enzyme loaded ferritins could form three-dimensional arrays with gold nanoparticles. Such developments indicate a great future for ferritins in the generation of adaptive and responsive systems, for example in responsive artificial organelle development. Demonstrating the application of ferritins as artificial organelles even further are recent reports of therapeutic use of enzyme-loaded ferritins. SOD-loaded ferritins have been delivered to caveolae where they ended up in the endosomes of endothelial cells.<sup>[145]</sup> In a mice model, the artificial organelles provided an anti-inflammatory effect due to the SOD activity. In another study a cytochrome C loaded ferritin has been delivered to the acute promyelocytic leukemia NB4 cell line *in vitro*.<sup>[146]</sup> In this system the activity of cytochrome C induced apoptosis of the cancer cells, indicating that ferritin-based artificial organelles could be used in the future for therapeutic applications.

Chaperonins are another class of protein nanocages that are used in nanoreactor development. For example, the thermosome (THS) has been used to encapsulate a  $Cu^{II}$ -catalyst<sup>[147]</sup> or HRP<sup>[148]</sup> to catalyze atom-transfer radical polymerization reactions yielding very monodisperse polymers. These reactions benefitted from the capability of THS to use ATP in order to cycle between open and closed states, allowing macromolecules, e.g. polymers, to leave the cage interior. In addition, by coating the two cavities of THS with dendritic poly(amidoamine) very monodisperse gold nanoparticles could be biomineralized with diameters of  $4.0 \pm 1.5$  and  $2.4 \pm 1.0$  nm.<sup>[149]</sup> These examples demonstrate that the THS cavities are compatible with both metals and enzymes, which could be useful for further development of these nanoreactors into various artificial organelles. The barrel-shaped interior of another chaperone, GroEL, could also be used for such applications since it can accommodate iron catalysts in a hemin form.<sup>[150-152]</sup> The peroxidase mimicking activity of the resulting nanoreactors has been used for the colorimetric<sup>[150]</sup> and chromogenic<sup>[151]</sup> detection of  $H_2O_2$ , glucose and catechol, but also for the oxidation of

homovanillic acid,<sup>[152]</sup> which is of course more interesting from an artificial organelle point of view.

#### 4. Artificial Organelles Produced *in Vivo*

The usage of protein-based nanoreactors offers another exciting prospect for the field of artificial organelles. Instead of incorporating premade nanoreactors, which will display transient activity, artificial organelles can be made *in situ* by employing the cell's own protein expression capacity. For this



**Figure 9.** Schematic representation of strategies leading to the *in vivo* production of protein-based artificial organelles. A) By tuning the properties of elastin-like proteins (ELPs), protein-based vesicles can be formed that can self-assemble intracellularly or can encapsulate enzymes *in vivo*. By combining both strategies *in vivo*, artificial organelle production could be achieved in the future. B) Proteinaceous organelles (encapsulins) are engineered to allow the *in vivo* formation and activity of artificial organelles. This can be done by attaching native cargo-sorting sequences to non-native cargo enzymes. C) Cage-like enzymes (lumazine synthases) are engineered into *in vivo* artificial organelles either by attaching the native cargo-sorting signal to non-native enzymes or by expansion of the protein cage and loading of (multiple) novel enzymes according to several *in vitro* and *in vivo* cargo-loading strategies. D) After removal of the genome from viral cages, these protein-based compartments can be loaded with (multiple) non-native enzymes by diverse engineered cargo-loading strategies. After further improvements of the self-assembly dynamics, *in vivo* cargo-loading, and the stability of the protein cage in the absence of the viral genome, *in vivo* artificial organelle production can be achieved. E) By computational *de novo* protein design novel artificial organelles with optimal features for specific catalytic applications are being developed in a bottom-up approach.



approach to be feasible both the capsule material and the cargo need to be produced by the cell and assembled together into an organelle with a clearly distinguishable functionality, for example catalytic activity. Preferably the reaction that is catalyzed is novel to the cell or restores or improves a native function. This *in vivo* approach requires the cell to produce all components, which has as a major benefit that the acquired functionality is inheritable and can be passed on to further generations. This however makes it of course also more challenging than *in vitro* approaches, as our current understanding of cell engineering towards the production of exogenous compounds is limited. Although in principle DNA-origami enzyme carriers<sup>[153,154]</sup> could be further developed into this direction as well, the biggest advancements in this strategy are made with protein-based systems (Figure 9), as protein engineering is well established, as will be described here in further detail. We will focus on those systems in which the most developments towards *in vivo* production of artificial organelles have been made and the progress towards *in cellulo* self-assembly, cargo loading, and catalytic activity will be described. Where it is applicable, we will discuss the added value that the artificial organelle (precursor) brings to cells or the catalytic process.

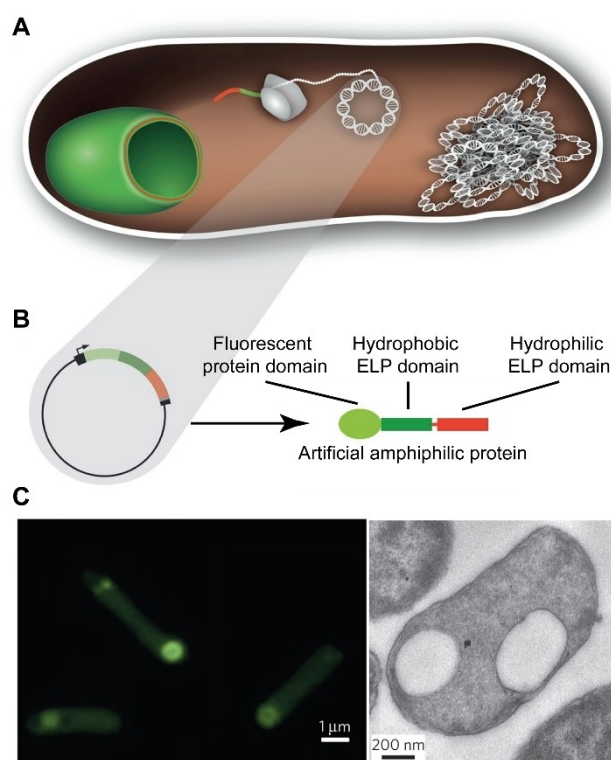
#### 4.1. ELP-based organelles: Protein-based organelles that mimic lipid vesicles

The protein-based structures that perhaps mimic the classical amphiphilic lipid-membrane structure the most are based on elastin-like polypeptides (ELPs; Figure 9A). As the name of these proteinaceous domains indicates, ELPs are derived from elastin, more precisely from its hydrophobic domains.<sup>[155]</sup> It has been established that repetitions of the VPGVG sequence present in these hydrophobic regions have stimulus-responsive coacervation behavior and can thus be reversibly switched between a water soluble state below their lower critical solution temperature (LCST) and a hydrophobic state above the LCST.<sup>[156]</sup> Most interestingly, this behavior can be tuned by ionic strength, length of the ELP domain, or by altering the fourth residue (guest residue) of the pentapeptide repeat. By constructing a diblock co-polypeptide in which the guest residues in the pentapeptide repeats were modified in such a way that a hydrophobic and a hydrophilic block were obtained, amphiphilic behavior was introduced that, under specific conditions, led to the *in vitro* self-assembly of the amphiphilic ELPs into several spherical micellar or vesicular particles.<sup>[157]</sup>

These ELP particles have been further developed into artificial organelle- or cell-like structures *in vitro*. For example, Schiller and co-workers have demonstrated that one set of assembly conditions can trigger the self-assembly of different ELP building blocks into protein membrane-based compartments (PMBCs) with tunable physicochemical properties.<sup>[158]</sup> Although these assembly conditions were not cell-like, such a strategy could work very well inside the cytosol where it is perhaps more difficult to trigger assembly based on changing conditions than in an *in vitro* setting. Interestingly, it was

demonstrated that the ELP membranes of these PMBCs can fuse with lipid membranes, forming protein-lipid hybrid membranes.<sup>[159]</sup> This could be very interesting for exchange between artificial and natural organelles or for mimicking vesicular transport. Furthermore, it was demonstrated that a wide variety of cargo molecules and proteins could be incorporated into the PMBCs,<sup>[158]</sup> which was used in the development of ELP-based protocells.<sup>[160]</sup> A T4 DNA ligase was encapsulated to mimic anabolic enzymatic reactions and a TEV protease was encapsulated or genetically fused to the amphiphilic membrane ELP as an example of catabolic activity. Adding to this *in vitro* functionality, Pirzer and co-workers have developed synthetic cells based on amphiphilic ELPs that are able to produce a functional RNA and protein and, most interestingly, to grow in an autonomous manner.<sup>[161]</sup> For this purpose, a cell-free transcription-translation system was encapsulated together with the DNA template encoding for an RNA aptamer, a fluorescent protein and the amphiphilic ELP. Incorporation of this ELP into the existing membrane allowed for vesicle growth. Such self-forming functionality could be a great advancement towards artificial organelles that can replicate together with their host cells.

Although most work described above is focused on creating ELP-based synthetic cells, ELP-based particles have also been

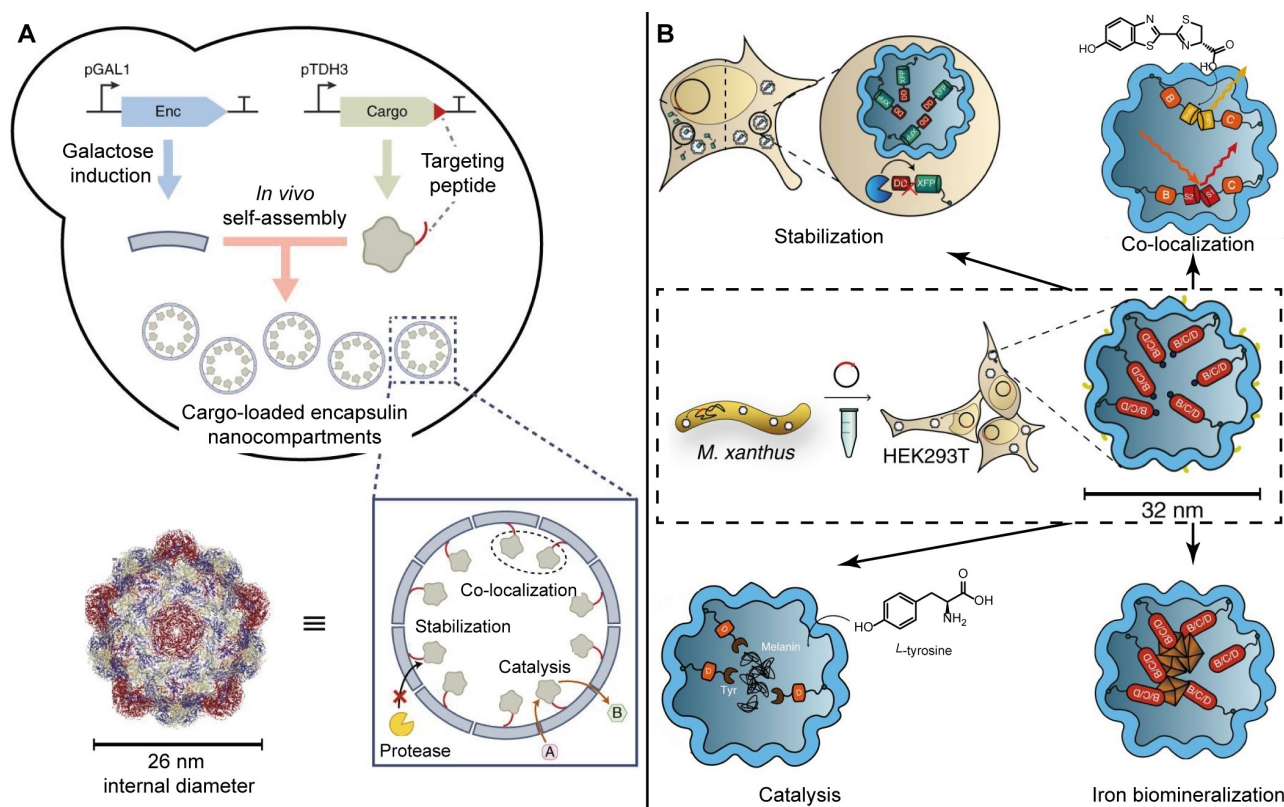


**Figure 10.** Overview of ELP compartments produced *in vivo*. A) Schematic representation of the production of a compartment (green) from plasmid DNA in *E. coli*. B) Schematic representation of the amphiphilic protein containing an N-terminal fluorescent domain and hydrophobic and hydrophilic ELP domains. C) Epifluorescence microscopy (left) and transmission electron microscopy (right) images of *E. coli* containing the ELP compartments as bright fluorescent spots (left) and clear regions (right). Figure adapted with permission from Ref. [162]. Copyright: 2014, Springer Nature.

employed inside *E. coli* cells (Figure 10).<sup>[162]</sup> Amphiphilic ELPs that were expressed in *E. coli* formed *in situ* organelle-like compartments with a membrane thickness of around 9 nm and a size that could be tuned between 40 nm and several hundred nanometers. In addition, the incorporation of the noncanonical amino acid *p*-azido-L-phenylalanine in the ELP sequence allowed for the *in vivo* functionalization of these compartments with for example a rhodamine dye. Furthermore, it was demonstrated that the ELP membranes interacted with the cellular membrane, which is again very promising for exchange and communication of the artificial organelle with the native system. Although no *in vivo* activity was established yet, the protein-encapsulation approaches used to generate ELP-based synthetic cells<sup>[160]</sup> could be used to incorporate active enzymes during self-assembly of the ELP compartments inside cells. Thus, their tunable properties, promising *in vitro* catalytic activity, and dynamic exchange behavior *in vivo* make ELP-based particles great candidates for further development into artificial organelles.

#### 4.2. Encapsulins: Engineering natural proteinaceous compartments into artificial organelles

In contrast to the ELP compartments described above, some protein-based compartments are already naturally existing in prokaryotes such as encapsulins, carboxysomes and the Pdu microcompartment.<sup>[4,5]</sup> Such compartments can be experimentally adapted to incorporate new functions or to be functional in higher-order organisms. Although some engineering into artificial organelles has been done with carboxysomes,<sup>[163,164]</sup> most of the developments in this field have been made with encapsulins. (Figure 9B). As such, these will be discussed here in further detail. Encapsulins are proteinaceous nanocompartments of 20–32 nm in size and are present in a great variety of bacteria and archaea as organelles that are involved in iron mineralization, oxidative and nitrosative stress resistance and anaerobic ammonium oxidation.<sup>[165]</sup> As such, a large number of cargo proteins are being targeted into the encapsulin core in nature. Quite recently, Sutter and co-workers discovered that this cargo sorting is being facilitated by a short C-terminal polypeptide tag on the cargo protein that can be recognized by a binding site on the interior of the encapsulin



**Figure 11.** Overview of encapsulin-based artificial organelles. A) *M. xanthus* encapsulin engineering into artificial organelles in *S. cerevisiae*. Attachment of the encapsulin-targeting peptide to cargo proteins results in encapsulation *in vivo* and thus the formation of artificial organelles that are catalytically active, bring multiple enzymes into close proximity and protect cargo enzymes from proteases.<sup>[178]</sup> B) *M. xanthus* encapsulin engineering into artificial organelles in HEK 293T cells. Heterologous protein expression results in the formation of the bacterial encapsulin loaded with its native cargo proteins in mammalian cells (middle panel). By attaching the encapsulation sequences of the native cargo proteins to non-native proteins, artificial organelles can be formed. These can be applied for *in vivo* stabilization of loaded proteins (top left), reconstitution of split-fluorescent and split-bioluminescent proteins (top right), iron biomineralization (bottom right), and even the formation of a melanosome that converts tyrosine into melanin (bottom left).<sup>[179]</sup> Figures adapted with permission from Ref. [178] and [179]. Copyright 2018: Lau et al. and Sigmund et al., respectively.

compartment.<sup>[166]</sup> This discovery revealed the potential for targeted sorting of exogenous cargoes inside these nanocompartments, making encapsulins great candidates for a plethora of applications in nanotechnology.<sup>[167]</sup> A variety of promising biomedical advancements have been made, such as the generation of iron-sequestering encapsulins that could function as electron microscopy gene reporters,<sup>[168]</sup> the formation of antimicrobial encapsulins that contain silver nanoparticles<sup>[169]</sup> or enhance the production of antimicrobial peptides,<sup>[170]</sup> and the modification of the encapsulin surface with photo-switchable fluorophores<sup>[171]</sup> or protection groups against protease degradation.<sup>[172]</sup> However, the focus below will be on developments that are beneficial for artificial organelle fabrication.

As encapsulins are protein-based nanocompartments that are naturally produced, there has not been a great necessity for capsid engineering in order to make them suitable for artificial organelle development. However, as the pores of native encapsulins are generally quite small, they might limit diffusion of substrates and products. Therefore, the pores of the *T. maritima* encapsulin have been enlarged from 3 Å to 11 Å by redesign of the pore-forming sequence.<sup>[173]</sup> Such an approach could be used to enhance the mass transport through other encapsulins as well and could thus be very fundamental for proper artificial organelle function.

Another approach to increase the catalytic possibilities of encapsulins is to diversify the cargoes that can be encapsulated. Various research groups have achieved this by creating genetic fusions of the specific sorting peptide and the cargo of interest and this has led to encapsulins that were loaded with various fluorescent or bioluminescent proteins *in vivo*<sup>[174–176]</sup> and *in vitro*.<sup>[176]</sup> Besides these model protein cargoes, also more functional proteins have been incorporated into encapsulins and even their *in vivo* functionality has been established. For example, it has been shown that teal fluorescent protein-loaded encapsulins can be taken up by macrophages, which demonstrates that encapsulins can be used to deliver cargo proteins to cells.<sup>[177]</sup> Most interestingly, encapsulin artificial organelle functionality has been described in both yeast<sup>[178]</sup> and mammalian cells,<sup>[179]</sup> demonstrating that these bacterial organelles can be used in higher order organisms as well (Figure 11). For the yeast system, Silver and co-workers expressed the *Myxococcus xanthus* encapsulin (EncMx) in *S. cerevisiae* together with various cargo proteins that were tagged with sorting peptides (Figure 11A).<sup>[178]</sup> They demonstrated that cargo proteins could be selectively encapsulated *in vivo*, which provided stabilization of a destabilized mNeonGreen protein against proteolytic degradation and allowed for the activation of a split-Venus fluorescent protein upon colocalization in the encapsulin core. Furthermore, an encapsulated Aro10p enzyme was catalytically active *in vitro*. Independently, Westmeyer and co-workers have used the same EncMx for the generation of synthetic compartments in HEK293T cells (Figure 11B).<sup>[179]</sup> Again selective *in vivo* encapsulation of heterologous cargo proteins was demonstrated as well as stabilization of a destabilized mEos4b fluorescent protein and colocalization of a split-PAmCherry-1. In addition, the enzymatic activities of a split-luciferase and a

tyrosinase, and iron biomineralization were established *in cellulo*. Thus, these encapsulin systems display many of the properties that are essential for further artificial organelle development.

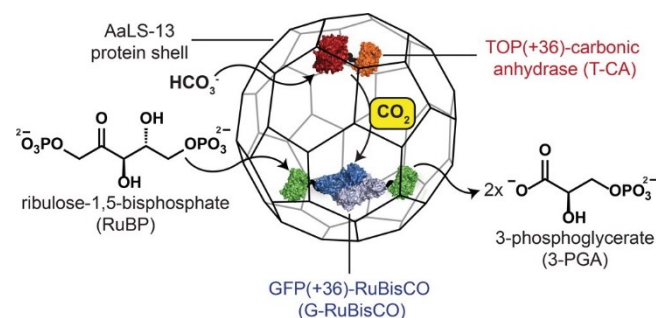
### 4.3. Lumazine synthases: engineering intracellular protein cages into artificial organelles

Besides encapsulins, there are many other protein-based cage structures that can be used for artificial organelle development. Another protein cage that has been exploited extensively, also *in vivo*, is lumazine synthase (LS; Figure 9C). Naturally, this enzyme is found in plants and many microorganisms, where it is involved in the biosynthesis of riboflavin.<sup>[180]</sup> Most interestingly, in some organisms this enzyme does not only function in the catalytic pathway by providing catalytic activity, but also by encapsulating the subsequent riboflavin synthase (RS) and thereby enhancing the overall reaction rate. This cage-like property of certain LS variants has been used to develop versatile nanoreactors.<sup>[181–187]</sup> For example, the LS from *Bacillus subtilis* (BsLS) has been loaded with non-native proteins and enzymes via specific recognition tags.<sup>[181]</sup> These tags were derived from the C-terminal domain of the native guest RS and allowed cargo sorting during cargo and capsid protein coproduction in *E. coli*. In addition, after purification of the loaded BsLS capsids, subtle pH and buffer changes could allow cargo dissociation and subsequent expansion of the BsLS capsid resulting in cargo release, which is promising for future responsive *in vivo* cargo-release systems. Another *in vitro* cargo release system was generated by genetic incorporation of a cysteine in the interior of the *Aquifex aeolicus* LS (AaLS).<sup>[182]</sup> Small molecule cargoes could be loaded via disulfide bonding and later released by reduction of the disulfide bond. Although such responsive release is very interesting for drug delivery approaches as the reducing environment of the cytosol would result in cargo release, it is not very beneficial for *in vivo* artificial organelle development as it could hamper encapsulation *in cellulo*.

The AaLS protein cage has been extensively engineered by Hilvert and co-workers.<sup>[180]</sup> For example, the size of the capsid has been expanded greatly from an external diameter of 15 nm to 39 nm by the introduction of negatively charged residues on the luminal surface.<sup>[183,188]</sup> As the internal volume increased 58 times by this size increase, such enlargement allows for the incorporation of larger proteins or increased numbers of cargo, which could enhance the enzymatic load of artificial organelles. Besides increasing the size of the AaLS nanocage, Hilvert and co-workers have focused on finding ways to tailor the morphology of assembled structures.<sup>[189]</sup> For this purpose, they made circularly permuted variants of the native AaLS protein that could self-assemble into tubular or spherical structures in *E. coli*. In addition, the modified AaLS proteins could coassemble together with the wild-type or other modified AaLS proteins, allowing for a high degree of control over the final properties of the capsid. This could be great for tailoring capsid properties to optimize catalytic functions of artificial organelles.

In addition to these structural improvements, a very efficient cargo-loading strategy has also been developed, similar to what has been described for ferritin in Section 3. For this purpose, the anionic residues on the interior face of the AaLS-13 capsid were employed as they can facilitate the *in vitro* encapsulation of oppositely charged cargo proteins, which for example, led to up to 100 complementary charged GFP(36+) molecules per capsid.<sup>[183]</sup> These charge interactions were further used to encapsulate two fluorescent proteins at once,<sup>[184]</sup> or to (co-) encapsulate active enzymes by creating a genetic fusion between the positively charged GFP(36+) and the specific enzyme(s).<sup>[185–187]</sup> While this charge-based encapsulation approach led to the encapsulation of approximately 45 enzymes per capsid, the confined environment of the AaLS cages did not increase the enzyme activity.<sup>[185,186]</sup> The same trend was found for a dual-enzyme AaLS-based carboxysome mimic (Figure 12), as co-encapsulation of ribulose-1,5-bisphosphate carboxylase/oxygenase (RuBisCO) and carbonic anhydrase (CA) did not enhance the catalytic efficiency of the pathway.<sup>[187]</sup> Nonetheless, enzyme function can be improved by encapsulation inside the AaLS nanocage as a result of protein protection against degradation. In addition, the charge complementarity could even be used to create capsid-in-capsid structures where positively supercharged ferritins were encapsulated inside the AaLS-13 cavity.<sup>[190]</sup> This could be great for creating new artificial organelle architectures, possibly similar to mitochondria with a luminal and intermembrane compartment. Furthermore, the encapsulation approach based on complementary charges could be feasible for *in vivo* capsid loading as a similar strategy employing deca-arginine (R10) tags instead of the GFP(36+) tag was already successful in *E. coli*.<sup>[191]</sup>

Most interestingly, this R10 tag system was used in *E. coli* to increase the loading of AaLS capsids with the cytoplasmically toxic HIV protease via directed evolution of the AaLS capsid protein.<sup>[192]</sup> Not only does this work demonstrate that *in cellulo* loading with an active enzyme is possible, but also that engineering approaches can increase the loading capacity further, possibly for each specific enzyme. Together, the



**Figure 12.** Schematic representation of an AaLS-based carboxysome mimic. The CA and RuBisCO enzymes are tagged with two different supercharged fluorescent proteins and encapsulated into the AaLS-13 protein cage through electrostatic interactions to yield nanoreactors with CO<sub>2</sub>-fixating activity as demonstrated by the conversion of hydrogen carbonate and ribulose-1,5-bisphosphate into two molecules of 3-phosphoglycerate. Figure reproduced with permission from Ref. [187]. Copyright: 2016, American Chemical Society.

modifications that have been made in the AaLS capsid illustrate how protein cages with a specific function in nature can be modified to adopt a new function. Such findings are great for future artificial organelle development both from AaLS capsids and from other protein cages.

#### 4.4. Virus capsids: Repurposing protein cages into artificial organelles

Virus capsids, the sturdy protein shells of viruses and bacteriophages, comprise another class of protein-based nanocompartments that are abundant in nature and are being applied for nanoreactor engineering.<sup>[115,135]</sup> In large contrast to encapsulins, virus capsids don't already have a function as organelles, but are instead well-equipped to protect their viral genome and infect a particular host. Nonetheless, they form robust protein cages in a predictable manner, making them great for engineering into artificial organelles (Figure 9D). The focus in this field has been on controlling the stability and assembly of the capsids, cargo incorporation mechanisms and more recently even on the incorporation of these systems inside living cells.

In 2007, the first nanoreactor was created from a virus by loading cowpea chlorotic mottle virus (CCMV) capsids with horseradish peroxidase.<sup>[193]</sup> As this viral capsid can be reversibly assembled by a pH switch, the cargo enzyme could be incorporated by mixing it with disassembled coat proteins *in vitro* and subsequently lowering the pH to 5.0 to trigger assembly into 28 nm capsids with  $T=3$  icosahedral symmetry. Since then, the focus in the CCMV field has been on development of more specific and efficient cargo incorporation strategies,<sup>[194–197]</sup> as well as on improving capsid assembly and stability under *in vivo* conditions.<sup>[198–200]</sup> Enzyme loading into CCMV capsids has been improved by the use of peptide coiled-coil interactions,<sup>[194,195]</sup> genetic fusion,<sup>[195]</sup> covalent attachment of cargo to the capsid interior by a Sortase A enzyme,<sup>[196]</sup> and single-stranded DNA tags.<sup>[197]</sup> In most of these strategies the N terminus of the CCMV coat protein, which is located on the capsid interior and normally interacts with the viral RNA, was modified to enable more specific and efficient cargo loading. Although none of the described cargo-loading methods have been employed *in vivo* yet, the modularity of the used systems allows for great flexibility once encapsulation is achieved *in vivo*.

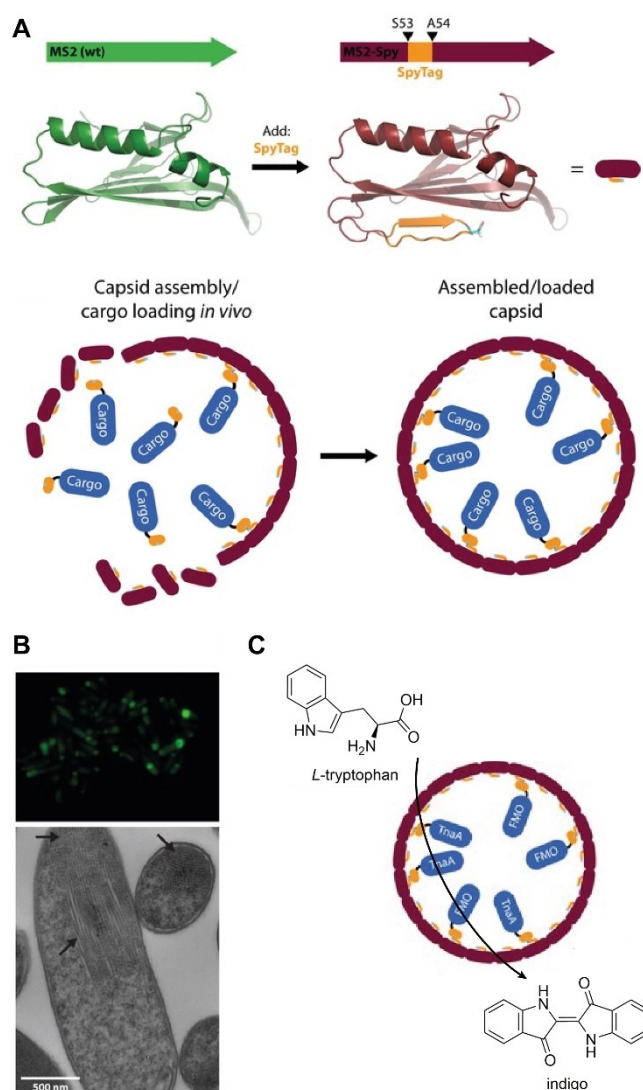
Besides the *in vitro* capsid loading strategies described above, important steps have been taken towards the *in vivo* use of CCMV nanoreactors by improving capsid assembly and stability under physiological conditions. For this purpose, a protein block copolymer consisting of the CCMV coat protein and an N-terminally fused ELP domain was generated.<sup>[198]</sup> By making use of the stimulus-responsive behavior of the incorporated ELP, assembly of 18 nm CCMV capsids with  $T=1$  icosahedral symmetry could be achieved above a certain temperature or ionic strength at physiological pH, without affecting the natural pH-induced capsid self-assembly. Further optimization of the ELP sequence allowed for capsid assembly at nearly-physiological conditions<sup>[199]</sup> and enhanced stability of

the resulting capsids.<sup>[200]</sup> Most importantly, one of the ELP-CCMV variants could be isolated from *E. coli* in a self-assembled state, indicating that the ELP domain stabilizes empty CCMV capsids to such an extent that self-assembly *in vivo* could be possible. In addition, although CCMV nanoreactors have not yet been used as artificial organelles *in vivo*, promising developments towards therapeutic use of these capsids<sup>[201]</sup> indicate that *in vivo* use is feasible. Hence, combining the discussed enzyme loading and cargo-independent capsid stabilization strategies could lead to CCMV-based artificial organelles in the future.

In addition to the plant virus CCMV, several bacteriophages have been engineered into artificial organelle (precursors). Since these are already present and stable inside bacteria, the focus of engineering of these cages has been mostly on finding methods to incorporate useful cargo enzymes. For example, the bacteriophage Q $\beta$  was loaded by the attachment of RNA tags to cargo enzymes.<sup>[202]</sup> These RNA tags consisted of the Q $\beta$  genome packaging hairpin that interacted with the interior of the Q $\beta$  capsid and an  $\alpha$ -Rev aptamer that could bind to a Rev-tag attached to the cargo enzyme. By co-expression of the Q $\beta$  coat protein, the RNA tag and the Rev-tagged enzyme, cargo loading was achieved *in vivo*. More importantly, encapsulation of aspartate dipeptidase E (PepE) enhanced the enzyme's thermostability and the PepE enzyme was protected from proteases. Furthermore, the modularity of this strategy allowed for the incorporation of a wide variety of cargo enzymes<sup>[203,204]</sup> and consequently their stabilization against a number of denaturing conditions<sup>[204]</sup> as well as for the combination of this approach with existing surface tagging methods,<sup>[205]</sup> which makes it great for the development of artificial organelles with a range of different functions.

Another bacteriophage that is being used for nanoreactor engineering is MS2. Enzyme incorporation into this 27 nm icosahedral protein cage has been achieved via charge interactions of the RNA-binding motif of the MS2 capsid protein with a DNA or polyanionic tag attached to the cargo enzyme.<sup>[206]</sup> In addition, the potential to regulate the inflow of substrates and the outflow of products by modification of the pore structure has been established.<sup>[207]</sup> Although these examples illustrate the great potential of MS2 engineering for nanoreactor development, the power of the MS2 capsid for artificial organelle production was actually demonstrated in a more recent report in which *in vivo* cargo loading and self-assembly of this protein cage were discussed (Figure 13).<sup>[208]</sup> In this work the SpyTag–SpyCatcher system<sup>[209]</sup> was employed to allow for specific cargo protein encapsulation. Genetic fusion of the SpyCatcher protein to two different cargo enzymes and of the SpyTag to an unstructured loop of the MS2 coat protein allowed for the formation of a covalent linkage between the cargo enzymes and the capsid interior in *E. coli* and subsequent loading of the capsids with a two-enzyme catalytic cascade.<sup>[208]</sup> This highly selective strategy led to an increase of the stability of the enzymes *in vitro* and more importantly enhanced the enzymatic activity of the full cascade with 60% *in vivo*.

Lastly, the bacteriophage P22 is being extensively studied for development into nanoreactors. The self-assembly of this capsid is slightly different than for the other virus-like particles



**Figure 13.** Schematic overview of MS2 based artificial organelles. A) *In vivo* cargo-loading strategy based on the introduction of a SpyTag into the MS2 interior and attachment of a SpyCatcher moiety to the cargo protein. B) Epifluorescence (top) and transmission electron (bottom) microscopy images of *E. coli* expressing MS2 compartments represented by bright fluorescent spots (top, mNeongreen) or arrows (bottom). C) MS2 organelles loaded with tryptophanase TnaA and (NADPH)-dependent flavin-containing monooxygenase catalyze the formation of indigo from L-tryptophan *in vivo*. Figures reproduced with permission from Ref. [208]. Copyright: 2016, Wiley-VCH.

(VLPs) discussed above, since the assembly of the 420 identical coat proteins is templated around 100 to 330 copies of a specific scaffold protein (SP) and results in the formation of a 58 nm procapsid with  $T=7$  icosahedral symmetry.<sup>[210,211]</sup> Interestingly, only a small portion of the scaffold protein is essential for templating capsid formation and the genetic fusion of this short domain to a variety of enzymes has resulted in the generation of a range of nanoreactors with assorted functionalities.<sup>[210–215]</sup> A very interesting nanoreactor among these was loaded with a three-enzyme cascade, stressing the power of the P22 capsid for binding enzymes together in a

confined environment.<sup>[214]</sup> An alternative approach that has been applied in order to achieve co-encapsulation employs genetic fusions of the individual enzymes to scaffold proteins, which was successful for a two-subunit enzyme<sup>[212]</sup> and co-incorporation of a ferritin cage together with an enzyme.<sup>[216]</sup> These examples demonstrate the potential of the P22 capsid for artificial organelle development as specific cargo encapsulation can be achieved in *E. coli* and different strategies have been developed to bring catalysts or pathways together. Nevertheless, enzyme activity has not yet been studied *in vivo*.

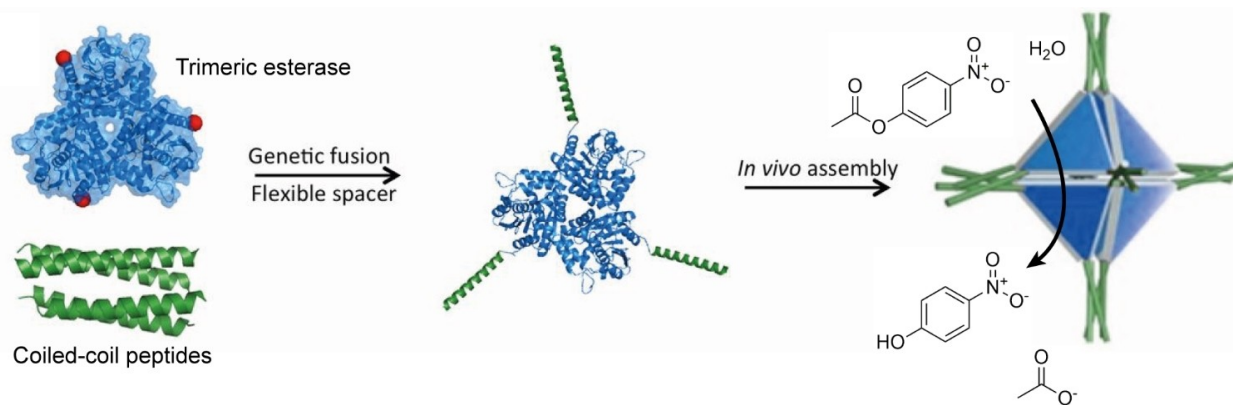
The focus of P22 research has not only been on cargo encapsulation, but the dynamics and stability of the assembled capsids<sup>[210,211,217,218]</sup> as well as *in vitro* cargo retention, release and incorporation<sup>[219–221]</sup> have been extensively studied as well. Interestingly, the isolated P22 capsid can undergo several rearrangements leading to cargo release upon temperature triggers.<sup>[210,211]</sup> Treatment with sodium dodecyl sulfate<sup>[217]</sup> or guanidine hydrochloride<sup>[219]</sup> can trigger the release from SP as well. Via these approaches the packaging density of the P22 capsids can be varied and the catalytic properties of an alcohol dehydrogenase (AdhD) have been controlled.<sup>[221]</sup> Although the demonstrated control over P22 dynamics and interior density can be quite easily translated into control over catalytic activity under *in vitro* conditions, the requirement for high temperatures and high chemical concentrations does not quite work for *in vivo* studies. A recent report on controlled release of cargo and SP from P22 capsids has focused on factors that are more feasible *in vivo*.<sup>[220]</sup> In this report, it was demonstrated that cargo release or retention from P22 capsids is dependent on a combination of electrostatic interactions and compatibility of cargo size and pore size. Therefore, by tuning the ionic strength, cargo pI, SP size and P22 pore size conditions could be found to favor cargo retention or release. Such a strategy could possibly be translated into an *in vivo* approach in which P22 artificial organelles can be assembled inside cells and subsequently their activity can be tuned.

All together, these results with viral cages demonstrate the great engineering potential that has been employed to reprogram natural protein cages into artificial organelles. Although every VLP has its own advantages, such as the reversible self-assembly of CCMV and the great thermostability of Q $\beta$ , and challenges, such as the stabilization of CCMV *in vivo* and the enhancement of dynamics of P22, some engineering approaches can be applied for multiple VLPs. For example, the *in vivo* cargo loading approach established for MS2<sup>[208]</sup> could be adopted to other VLPs as well. Moreover, the ELP stabilization method used for CCMV<sup>[198–200]</sup> could be employed to make the self-assembly of other VLPs more tunable. One challenge that remains for VLP-based artificial organelles in general is the lack of knowledge on the advantage of enzyme encapsulation inside these protein cages *in vivo* compared to free enzymes. Therefore, future research should focus on establishing *in vivo* catalytic activity of the new artificial organelles. Thus, by combining the already established engineering strategies with new approaches to overcome common challenges, artificial organelle development from viral capsids can forward greatly in the future.

#### 4.5. Designed protein cages: building protein-based artificial organelles completely from the bottom up

In addition to engineering already existing organelles or protein cages into artificial organelles, one can also consider designing and constructing completely new organelles (Figure 9E). Despite the fact that this approach requires a considerable understanding of the factors involved in protein self-assembly into complex structures<sup>[222]</sup> as well as tremendous computing power, recent advances in computer-aided *de novo* protein design<sup>[223]</sup> have paved the road for the development of protein cages from scratch.<sup>[224–228]</sup> Although most of the progress in this research field has been focused on assembly and stability of the protein cage itself, promising developments have led to the introduction of catalytic activity or to the production of designed protein cages *in vivo*.

Initially, Yeates and co-workers established that symmetry and geometry are two essential parameters in the design of self-assembling protein cages.<sup>[225,229]</sup> They established the formation of a tetrahedral protein cage by creating a genetic fusion of two multimeric proteins that were connected by an  $\alpha$ -helical domain. In this system the multimeric proteins determine the symmetry, while the rigidity of the  $\alpha$ -helix provides the geometrical control necessary to favor a tetrahedral cage structure. Further improvements of this system focusing on computer-aided design by the Yeates and Baker labs have led to the design and formation of various additional protein cages<sup>[224,228,230,231]</sup> and more recently to the formation of two megadalton scale protein cages with two<sup>[227]</sup> or three<sup>[232]</sup> symmetry elements. This is a great achievement as these cages are of similar size as the viral cages described above and it stresses the importance of combining computer power and an extensive understanding of the biochemistry involved. In a slightly different approach March and co-workers have used (combinations of multimeric proteins and) multimeric  $\alpha$ -helical coiled-coil peptides to design and build novel protein cages.<sup>[233–237]</sup> Such an approach can be beneficial as coiled-coil engineering can be used to create more different symmetry axes and it is not limited to oligomerization domains that nature provides us with. In general, these developments in the designed protein cages field hold great promise for artificial organelle development as it might in the future become possible to tailor-make protein cages for specific catalytic purposes. Furthermore, protein cages can be optimized to have beneficial self-assembly dynamics inside a specific cell type. Although there are still some challenges such as solubility issues to overcome,<sup>[228]</sup> and most of the above mentioned reports are mainly focused on the design of protein cages, there have already been a few promising results regarding functionalization of these designed cages.<sup>[224,226,235,238,239]</sup> For example, the model protein GFP has been incorporated into a designed icosahedron by genetic fusion to the cage monomers.<sup>[224]</sup> Interestingly, the size of the entrance and exit channels of this designed cage could be controlled by the addition of a designed protein pentamer, which could be used in the future to modulate influx and efflux of substrates and products, respectively. Another designed cage contained esterase activity



**Figure 14.** Schematic representation of a self-assembling de novo designed octahedral protein cage. Self-assembly is based on a trimeric esterase and tetrameric coiled-coil peptides that are genetically fused via flexible spacers. Esterase activity is maintained *in vitro* upon self-assembly, as demonstrated by hydrolysis of *p*-nitrophenyl acetate. Figure reproduced with permission from Ref. [235]. Copyright: 2016, National Academy of Sciences.

as a trimeric esterase was employed as one of the symmetry-inducing components (Figure 14).<sup>[235]</sup> Although the specific activity was slightly reduced compared to the free esterase, the fact that activity was maintained indicates that the esterase tertiary structure is not altered during assembly into the cage structure. In another striking example, designed protein cages have been used as a scaffold to bring two cellulase enzymes together, enhancing the overall speed of cellulose degradation.<sup>[238]</sup> This work could be easily extended to bring other combinations of enzymes together and enhance the overall activity of their catalytic pathway.

Most interestingly, designed protein cages have already been used *in vivo*. These so-called protein-origami cages (Figure 15A) have been produced by using one single protein chain containing coiled-coil staple regions<sup>[239,240]</sup> in a similar fashion as for DNA origami.<sup>[241]</sup> Although this self-assembly approach is somewhat different from most protein cage systems, for example, in that it is not the product of self-assembly of identical building blocks, it is very promising for further development because of lesser importance of symmetry and thus more freedom in the design. Moreover, a split fluorescent protein as well as an activatable split-luciferase could be incorporated in the coiled-coil protein origami (CCPO) cages, demonstrating the feasibility of protein encapsulation and functional assembly within these structures.<sup>[239]</sup> Another important feature that makes these CCPOs great candidates for artificial organelle development is the fact that they can self-assemble in both bacterial and mammalian cells as well as in living mice (Figure 15B,C), while maintaining luciferase activity and without introducing any toxicity.

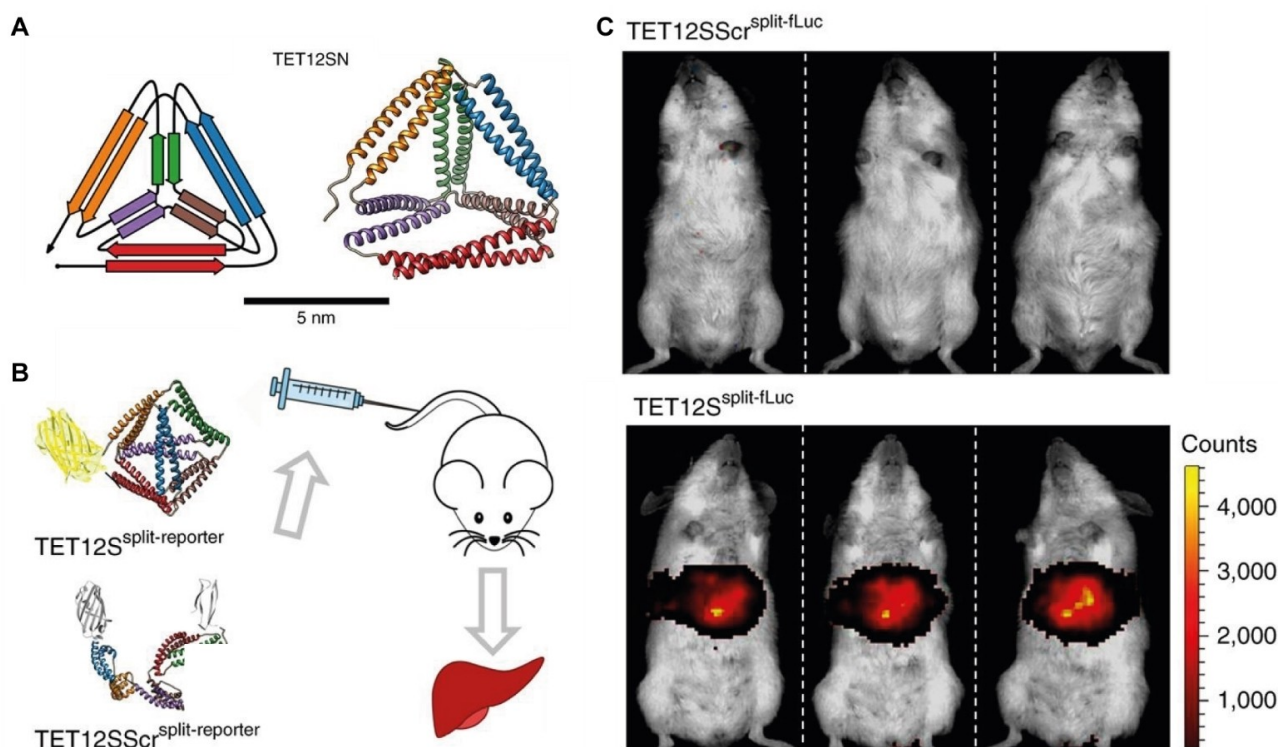
Therefore, although this is still an emerging field, designed protein cages can be very instrumental in artificial organelle development. Especially the plethora of design features that can be included is very promising. For example, protein cages can be designed in a scalable<sup>[242]</sup> or adaptable<sup>[243]</sup> manner by incorporating split inteins or disulfide interactions, respectively. Alternatively, capsid assembly can be controlled allosterically<sup>[244]</sup> or via chemical, thermal and redox control over metal

coordination.<sup>[245]</sup> By using and exploring all of these features, our understanding of these strategies grows and the road towards designed artificial organelles is paved. In addition, this knowledge can be potentially used to engineer existing protein cages in order to achieve optimal properties for a specific artificial organelle. The extent of expertise that has been developed on the design of self-assembling proteins can be instrumental for gaining control over the specific properties of protein cages in such a way that researchers are no longer limited to the features that nature provides us with. Together with, for example, developments in *de novo* design of enzymes,<sup>[246,247]</sup> designer protein cages could allow for the development of completely new organelles perfectly optimized for their specific function.

## 5. Summary and Outlook

Artificial organelle research has taken a great flight in recent years. In this truly multidisciplinary field, in which catalysis, chemical biology, nanoscience and synthetic biology are combined, designer compartments have been developed that are integrated with cells to add novel functionality. Although progress is highly promising, there are still many challenges ahead before its full potential is reached.

Considerable progress has been made in the development of catalytic systems based on transition metals that show activity in the interior of living cells. The advantage of organometallic catalysts over enzymes is that the vast array of reactions that occur in cells can be expanded with abiotic reactions. Though, most examples rely on deprotection reactions, whereas C–C bond formations are under-represented. These abiotic reactions offer a strategy for targeted prodrug activation. That is, if the fate of the catalyst can be controlled. Another challenge lies in the biocompatibility of the catalytic systems. Most complexes are fairly toxic to cells, and their lifetimes are short due to the reactive cellular environment. Compartmentalization in synthetic polymeric assemblies can be



**Figure 15.** A self-assembling de novo designed tetrahedral protein cage *in vivo*. A) The protein-origami cage (TET12SN) design is based on a single protein strand containing coiled-coil regions. B) The two halves of a split-luciferase are attached to both ends of the protein-origami strands, allowing reconstitution of bioluminescence upon formation of the protein cage (TET12S<sup>split-reporter</sup>). As a negative control, the sequence of the protein origami strand is scrambled (TET12SScrl<sup>split-reporter</sup>) to prevent protein cage formation and reconstitution of bioluminescence. Hydrodynamic delivery of plasmids allows for expression of the artificial organelle in the liver, which can be monitored by the luciferase activity. C) *In vivo* imaging based on split-luciferase reconstitution demonstrating bioluminescent activity in the liver only when the plasmid for the correctly folding TET12S cage was delivered. Figure reproduced with permission from Ref. [239]. Copyright: 2017, Springer Nature.

a means to address some of the challenges. Encapsulation of catalysts in nano-assemblies could provide protection to reach longer lifetimes and meanwhile limit toxicity by minimizing undesired effects such as interactions with DNA or enzymes. It could also boost catalytic activity, as high local concentrations of catalyst can be reached within a confined space. Additionally, the assemblies can be functionalized to enhance cellular uptake and specifically target certain tissues, without altering the properties of the catalyst. As of now, compartmentalization strategies are rare for organometallic catalysts, especially when compared to enzyme nanoreactors. There is still much to gain from a better compartment design to allow a more effective integration in living cells. It would be even more versatile when chemo-enzymatic catalytic cascades could be stably integrated, as this would further extend our synthetic capacity *in cellulo*. With this toolbox, it would be possible to add designer pathways to cells with actual function beyond the conceptual approaches that have been now mostly described.

Until now, artificial organelles display merely a static function; their activity *in cellulo* cannot be regulated. This is in sharp contrast to regular cellular processes which respond to many feedback mechanisms. The development of transient nanoreactors, of which the activity can be switched on or off, would therefore be an important step forward toward more

life-like behavior. This could for example be achieved by creating polymer nanoreactors with a stimulus-responsive shell, or with *in vivo* expressed protein cages of which the protein units contain activatable degradation tags.

Besides transient regulation, also spatial control is of interest. There is only limited control over where the artificial organelles end up in the cell. For their optimal activity it would be useful to bring them into close proximity of certain natural organelles such as the mitochondria. Although some rudimentary methods have been employed for synthetic organelles, for *in cellulo* expressed systems this remains an unexplored approach.

Finally, the ideal artificial organelle will be copied along during cell division and will add orthogonal catalytic activity to living cells. The former aspect can be only achieved using *in cellulo* production, whereas the latter is the realm of the premade artificial organelles. Although a combination of these features therefore seems to be a distant future, with the advance of protein designer cages and our ability to develop protein-based ligands for organometallic complexes, a more intimate integration of the two artificial organelle classes should be conceptually feasible.



## Acknowledgements

The authors would like to acknowledge the ERC Advanced grant Artisym 694120 and the Dutch Ministry of Education, Culture and Science (Gravitation program 024.001.035) for funding.

## Conflict of Interest

The authors declare no conflict of interest.

**Keywords:** artificial organelles · intracellular catalysis · nanoreactors · nanotechnology · synthetic biology

- [1] L. Sagan, *J. Theor. Biol.* **1967**, *14*, 225–274.
- [2] D. Bracha, M. T. Walls, C. P. Brangwynne, *Nat. Biotechnol.* **2019**, *37*, 1435–1445.
- [3] C. D. Reinkemeier, G. E. Girona, E. A. Lemke, *Science* **2019**, *363*, eaaw2644.
- [4] T. O. Yeates, C. A. Kerfeld, S. Heinhorst, G. C. Cannon, J. M. Shively, *Nat. Rev. Microbiol.* **2008**, *6*, 681–691.
- [5] A. Hagen, M. Sutter, N. Sloan, C. A. Kerfeld, *Nat. Commun.* **2018**, *9*, 2881.
- [6] D. E. Cane, *Science* **1998**, *282*, 63–68.
- [7] J. E. Dueber, G. C. Wu, G. R. Malmirchegini, T. S. Moon, C. J. Petzold, A. V. Ullal, K. L. J. Prather, J. D. Keasling, *Nat. Biotechnol.* **2009**, *27*, 753–759.
- [8] Z. Zhao, J. Fu, S. Dhakal, A. Johnson-Buck, M. Liu, T. Zhang, N. W. Woodbury, Y. Liu, N. G. Walter, H. Yan, *Nat. Commun.* **2016**, *7*, 10619.
- [9] J. F. Mukerabigwi, Z. Ge, K. Kataoka, *Chem. Eur. J.* **2018**, *24*, 15706–15724.
- [10] A. P. M. Weber, K. W. Osteryoung, *Plant Physiol.* **2010**, *154*, 593–597.
- [11] B. C. Buddingh', J. C. M. van Hest, *Acc. Chem. Res.* **2017**, *50*, 769–777.
- [12] J. G. Rebelein, T. R. Ward, *Curr. Opin. Biotechnol.* **2018**, *53*, 106–114.
- [13] M. Martínez-Calvo, J. L. Mascareñas, *Coord. Chem. Rev.* **2018**, *359*, 57–79.
- [14] J. J. Soldevila-Barreda, N. Metzler-Nolte, *Chem. Rev.* **2019**, *119*, 829–869.
- [15] K. Vong, K. Tanaka in *Handbook of in Vivo Chemistry in Mice: From Lab to Living System*, Wiley, Hoboken, **2020**, pp. 309–353.
- [16] J. L. Mascareñas, P. Destito, C. Vidal, F. López, *Chem. Eur. J.* **2020**, DOI 10.1002/chem.202003927.
- [17] C. Andreini, I. Bertini, G. Cavallaro, G. L. Holliday, J. M. Thornton, *J. Biol. Inorg. Chem.* **2008**, *13*, 1205–1218.
- [18] M. A. Zoroddu, J. Aaseth, G. Crisponi, S. Medici, M. Peana, V. M. Nurchi, *J. Inorg. Biochem.* **2019**, *195*, 120–129.
- [19] P. Zhang, P. J. Sadler, *J. Organomet. Chem.* **2017**, *839*, 5–14.
- [20] J. A. Prescher, D. H. Dube, C. R. Bertozzi, *Nature* **2004**, *430*, 873–877.
- [21] J. A. Prescher, C. R. Bertozzi, *Nat. Chem. Biol.* **2005**, *1*, 13–21.
- [22] C. Streu, E. Meggers, *Angew. Chem. Int. Ed.* **2006**, *45*, 5645–5648; *Angew. Chem.* **2006**, *118*, 5773–5776.
- [23] M. I. Sánchez, C. Penas, M. E. Vázquez, J. L. Mascareñas, *Chem. Sci.* **2014**, *5*, 1901–1907.
- [24] G. Y. Tonga, Y. Jeong, B. Duncan, T. Mizuhara, R. Mout, R. Das, S. T. Kim, Y. C. Yeh, B. Yan, S. Hou, et al., *Nat. Chem.* **2015**, *7*, 597–603.
- [25] T. Völker, F. Dempwolff, P. L. Graumann, E. Meggers, *Angew. Chem. Int. Ed.* **2014**, *53*, 10536–10540; *Angew. Chem.* **2014**, *126*, 10705–10710.
- [26] M. Tomás-Gamasa, M. Martínez-Calvo, J. R. Couceiro, J. L. Mascareñas, *Nat. Commun.* **2016**, *7*, 12538.
- [27] C. Vidal, M. Tomás-Gamasa, P. Destito, F. López, J. L. Mascareñas, *Nat. Commun.* **2018**, *9*, 1913.
- [28] K. K. Sadhu, T. Eierhoff, W. Römer, N. Winssinger, *J. Am. Chem. Soc.* **2012**, *134*, 20013–20016.
- [29] J. Chen, K. Li, J. S. Shon, S. C. Zimmerman, *J. Am. Chem. Soc.* **2020**, *142*, 4565–4569.
- [30] M. Jeschek, R. Reuter, T. Heinisch, C. Trindler, J. Klehr, S. Panke, T. R. Ward, *Nature* **2016**, *537*, 661–665.
- [31] Y. Okamoto, R. Kojima, F. Schwizer, E. Bartolami, T. Heinisch, S. Matile, M. Fussenegger, T. R. Ward, *Nat. Commun.* **2018**, *9*, 1943.
- [32] S. Eda, I. Nasibullin, K. Vong, N. Kudo, M. Yoshida, A. Kurbangalieva, K. Tanaka, *Nat. Catal.* **2019**, *2*, 780–792.
- [33] K. E. Beatty, F. Xie, Q. Wang, D. A. Tirrell, *J. Am. Chem. Soc.* **2005**, *127*, 14150–14151.
- [34] V. Bevilacqua, M. King, M. Chaumontet, M. Nothisen, S. Gabillet, D. Buisson, C. Puente, A. Wagner, F. Taran, *Angew. Chem. Int. Ed.* **2014**, *53*, 5872–5876; *Angew. Chem.* **2014**, *126*, 5982–5986.
- [35] Y. Bai, X. Feng, H. Xing, Y. Xu, B. K. Kim, N. Baig, T. Zhou, A. A. Gewirth, Y. Lu, E. Oldfield, et al., *J. Am. Chem. Soc.* **2016**, *138*, 11077–11080.
- [36] J. Huang, L. Wang, P. Zhao, F. Xiang, J. Liu, S. Zhang, *ACS Catal.* **2018**, *8*, 5941–5946.
- [37] F. Wang, Y. Zhang, Z. Liu, Z. Du, L. Zhang, J. Ren, X. Qu, *Angew. Chem. Int. Ed.* **2019**, *58*, 6987–6992.
- [38] F. Xiang, B. Li, P. Zhao, J. Tan, Y. Yu, S. Zhang, *Adv. Synth. Catal.* **2019**, *361*, 5057–5062.
- [39] M. Martínez-Calvo, J. R. Couceiro, P. Destito, J. Rodríguez, J. Mosquera, J. L. Mascareñas, *ACS Catal.* **2018**, *8*, 6055–6061.
- [40] J. Li, J. Yu, J. Zhao, J. Wang, S. Zheng, S. Lin, L. Chen, M. Yang, S. Jia, X. Zhang, et al., *Nat. Chem.* **2014**, *6*, 352–361.
- [41] J. Wang, S. Zheng, Y. Liu, Z. Zhang, Z. Lin, J. Li, G. Zhang, X. Wang, J. Li, P. R. Chen, *J. Am. Chem. Soc.* **2016**, *138*, 15118–15121.
- [42] R. M. Yusop, A. Unciti-Broceta, E. M. V. Johansson, R. M. Sánchez-Martín, M. Bradley, *Nat. Chem.* **2011**, *3*, 239–243.
- [43] J. Clavdetscher, E. Indrigo, S. V. Chankeshwara, A. Lilienkamp, M. Bradley, *Angew. Chem. Int. Ed.* **2017**, *56*, 6864–6868; *Angew. Chem.* **2017**, *129*, 6968–6972.
- [44] M. Sancho-Albero, B. Rubio-Ruiz, A. M. Pérez-López, V. Sebastián, P. Martín-Duque, M. Arruebo, J. Santamaría, A. Unciti-Broceta, *Nat. Catal.* **2019**, *2*, 864–872.
- [45] M. A. Miller, B. Askevold, H. Mikula, R. H. Kohler, D. Pirovich, R. Weissleder, *Nat. Commun.* **2017**, *8*, 15906.
- [46] M. A. Miller, H. Mikula, G. Luthria, R. Li, S. Kronister, M. Prytyskach, R. H. Kohler, T. Mitchison, R. Weissleder, *ACS Nano* **2018**, *12*, 12814–12826.
- [47] F. Wang, Y. Zhang, Z. Du, J. Ren, X. Qu, *Nat. Commun.* **2018**, *9*, 1209.
- [48] R. Martínez, C. Carrillo-Carrión, P. Destito, A. Alvarez, M. Tomás-Gamasa, B. Pelaz, F. Lopez, J. L. Mascareñas, P. del Pino, *Cell Reports Phys. Sci.* **2020**, *1*, 100076.
- [49] B. M. Trost, M. U. Frederiksen, M. T. Rudd, *Angew. Chem. Int. Ed.* **2005**, *44*, 6630–6666; *Angew. Chem.* **2005**, *117*, 6788–6825.
- [50] G. C. Vougioukalakis, R. H. Grubbs, *Chem. Rev.* **2010**, *110*, 1746–1787.
- [51] T. Kondo, Y. Morisaki, S. Y. Uenoyama, K. Wada, T. A. Mitsudo, *J. Am. Chem. Soc.* **1999**, *121*, 8657–8658.
- [52] S. Tanaka, H. Saburi, Y. Ishibashi, M. Kitamura, *Org. Lett.* **2004**, *6*, 1873–1875.
- [53] T. Völker, E. Meggers, *ChemBioChem* **2017**, *18*, 1083–1086.
- [54] R. Das, R. F. Landis, G. Y. Tonga, R. Cao-Milán, D. C. Luther, V. M. Rotello, *ACS Nano* **2019**, *13*, 229–235.
- [55] Y. Chen, A. S. Kamlet, J. B. Steinman, D. R. Liu, *Nat. Chem.* **2011**, *3*, 146–153.
- [56] K. K. Sadhu, N. Winssinger, *Chem. Eur. J.* **2013**, *19*, 8182–8189.
- [57] L. Holtzer, I. Oleinich, M. Anzola, E. Lindberg, K. K. Sadhu, M. Gonzalez-Gaitan, N. Winssinger, *ACS Cent. Sci.* **2016**, *2*, 394–400.
- [58] T. Vornholt, M. Jeschek, *ChemBioChem* **2020**, *21*, 2241–2249.
- [59] L. M. Gaetke, H. S. Chow-Johnson, C. K. Chow, *Arch. Toxicol.* **2014**, *88*, 1929–1938.
- [60] V. V. Rostovtsev, L. G. Green, V. V. Fokin, K. B. Sharpless, *Angew. Chem. Int. Ed.* **2002**, *41*, 2596–2599; *Angew. Chem.* **2002**, *114*, 2708–2711.
- [61] C. W. Tornøe, C. Christensen, M. Meldal, *J. Org. Chem.* **2002**, *67*, 3057–3064.
- [62] A. E. Speers, G. C. Adam, B. F. Cravatt, *J. Am. Chem. Soc.* **2003**, *125*, 4686–4687.
- [63] A. J. Link, D. A. Tirrell, *J. Am. Chem. Soc.* **2003**, *125*, 11164–11165.
- [64] A. J. Link, M. K. S. Vink, D. A. Tirrell, *J. Am. Chem. Soc.* **2004**, *126*, 10598–10602.
- [65] E. M. Sletten, C. R. Bertozzi, *Angew. Chem. Int. Ed.* **2009**, *48*, 6974–6998; *Angew. Chem.* **2009**, *121*, 7108–7133.
- [66] S. I. Presolski, V. Hong, S. H. Cho, M. G. Finn, *J. Am. Chem. Soc.* **2010**, *132*, 14570–14576.
- [67] K. E. Beatty, J. C. Liu, F. Xie, D. C. Dieterich, E. M. Schuman, Q. Wang, D. A. Tirrell, *Angew. Chem. Int. Ed.* **2006**, *45*, 7364–7367; *Angew. Chem.* **2006**, *118*, 7524–7527.
- [68] M. Sawa, T.-L. Hsu, T. Itoh, M. Sugiyama, S. R. Hanson, P. K. Vogt, C.-H. Wong, *Proc. Nat. Acad. Sci.* **2006**, *103*, 12371–12376.
- [69] T.-L. Hsu, S. R. Hanson, K. Kishikawa, S.-K. Wang, M. Sawa, C.-H. Wong, *Proc. Nat. Acad. Sci.* **2007**, *104*, 2614–2619.

- [70] A. Salic, T. J. Mitchison, *Proc. Nat. Acad. Sci.* **2008**, *105*, 2415–2420.
- [71] C. Y. Jao, A. Salic, *Proc. Nat. Acad. Sci.* **2008**, *105*, 15779–15784.
- [72] M. A. Breidenbach, J. E. G. Gallagher, D. S. King, B. P. Smart, P. Wu, C. R. Bertozzi, *Proc. Nat. Acad. Sci.* **2010**, *107*, 3988–3993.
- [73] V. Hong, S. I. Presolski, C. Ma, M. G. Finn, *Angew. Chem. Int. Ed.* **2009**, *48*, 9879–9883; *Angew. Chem.* **2009**, *121*, 10063–10067.
- [74] D. Soriano Del Amo, W. Wang, H. Jiang, C. Besanceney, A. C. Yan, M. Levy, Y. Liu, F. L. Marlow, P. Wu, *J. Am. Chem. Soc.* **2010**, *132*, 16893–16899.
- [75] C. Besanceney-Webler, H. Jiang, T. Zheng, L. Feng, D. Soriano Del Amo, W. Wang, L. M. Klivansky, F. L. Marlow, Y. Liu, P. Wu, *Angew. Chem. Int. Ed.* **2011**, *50*, 8051–8056; *Angew. Chem.* **2011**, *123*, 8201–8206.
- [76] W. Wang, S. Hong, A. Tran, H. Jiang, R. Triano, Y. Liu, X. Chen, P. Wu, *Chem. Asian J.* **2011**, *6*, 2796–2802.
- [77] V. Hong, N. F. Steinmetz, M. Manchester, M. G. Finn, *Bioconjugate Chem.* **2010**, *21*, 1912–1916.
- [78] D. C. Kennedy, C. S. McKay, M. C. B. Legault, D. C. Danielson, J. A. Blake, A. F. Pegoraro, A. Stolow, Z. Mester, J. P. Pezacki, *J. Am. Chem. Soc.* **2011**, *133*, 17993–18001.
- [79] H. Jiang, T. Zheng, A. Lopez-Aguilar, L. Feng, F. Kopp, F. L. Marlow, P. Wu, *Bioconjugate Chem.* **2014**, *25*, 698–706.
- [80] Z. Hao, Y. Song, S. Lin, M. Yang, Y. Liang, J. Wang, P. R. Chen, *Chem. Commun.* **2011**, *47*, 4502–4504.
- [81] C. Uttamapinant, A. Tangpeerachaikul, S. Grecian, S. Clarke, U. Singh, P. Slade, K. R. Gee, A. Y. Ting, *Angew. Chem. Int. Ed.* **2012**, *51*, 5852–5856; *Angew. Chem.* **2012**, *124*, 5954–5958.
- [82] W. S. Brotherton, H. A. Michaels, J. Tyler Simmons, R. J. Clark, N. S. Dalai, L. Zhu, *Org. Lett.* **2009**, *11*, 4954–4957.
- [83] J. Clavadetscher, S. Hoffmann, A. Lilienkamp, L. Mackay, R. M. Yusop, S. A. Rider, J. J. Mullins, M. Bradley, *Angew. Chem. Int. Ed.* **2016**, *55*, 15662–15666; *Angew. Chem.* **2016**, *128*, 15891–15895.
- [84] K. C. Nicolaou, P. G. Bulger, D. Sarlah, *Angew. Chem. Int. Ed.* **2005**, *44*, 4442–4489; *Angew. Chem.* **2005**, *117*, 4516–4563.
- [85] A. Biffis, P. Centomo, A. Del Zotto, M. Zecca, *Chem. Rev.* **2018**, *118*, 2249–2295.
- [86] W. A. Herrmann, C. W. Kohlpaintner, *Angew. Chem. Int. Ed. Engl.* **1993**, *32*, 1524–1544.
- [87] K. H. Shaughnessy, *Eur. J. Org. Chem.* **2006**, 1827–1835.
- [88] A. L. Casalnuovo, J. C. Calabrese, *J. Am. Chem. Soc.* **1990**, *112*, 4324–4330.
- [89] H. Dibowski, F. P. Schmidtchen, *Angew. Chem. Int. Ed.* **1998**, *37*, 476–478; *Angew. Chem.* **1998**, *110*, 487–489.
- [90] D. T. Bong, M. R. Ghadiri, *Org. Lett.* **2001**, *3*, 2509–2511.
- [91] M. Vilaró, G. Arsequell, G. Valencia, A. Ballesteros, J. Barluenga, *Org. Lett.* **2008**, *10*, 3243–3245.
- [92] K. Kodama, S. Fukuzawa, H. Nakayama, T. Kigawa, K. Sakamoto, T. Yabuki, N. Matsuda, M. Shirouzu, K. Takio, K. Tachibana, et al., *ChemBioChem* **2006**, *7*, 134–139.
- [93] K. Kodama, S. Fukuzawa, H. Nakayama, K. Sakamoto, T. Kigawa, T. Yabuki, N. Matsuda, M. Shirouzu, K. Takio, S. Yokoyama, et al., *ChemBioChem* **2007**, *8*, 232–238.
- [94] S. D. Tilley, M. B. Francis, *J. Am. Chem. Soc.* **2006**, *128*, 1080–1081.
- [95] J. M. Chalker, C. S. C. Wood, B. G. Davis, *J. Am. Chem. Soc.* **2009**, *131*, 16346–16347.
- [96] J. H. Li, X. D. Zhang, Y. X. Xie, *Eur. J. Org. Chem.* **2005**, 4256–4259.
- [97] C. D. Spicer, B. G. Davis, *Chem. Commun.* **2011**, *47*, 1698–1700.
- [98] C. D. Spicer, T. Triemer, B. G. Davis, *J. Am. Chem. Soc.* **2012**, *134*, 800–803.
- [99] C. D. Spicer, B. G. Davis, *Chem. Commun.* **2013**, *49*, 2747–2749.
- [100] Z. Gao, V. Gouverneur, B. G. Davis, *J. Am. Chem. Soc.* **2013**, *135*, 13612–13615.
- [101] X. Ma, H. Wang, W. Chen, *J. Org. Chem.* **2014**, *79*, 8652–8658.
- [102] J. T. Weiss, J. C. Dawson, K. G. Macleod, W. Rybski, C. Fraser, C. Torres-Sánchez, E. E. Patton, M. Bradley, N. O. Carragher, A. Unciti-Broceta, *Nat. Commun.* **2014**, *5*, 3277.
- [103] M. O. N. van de L'Isle, M. C. Ortega-Liebana, A. Unciti-Broceta, *Curr. Opin. Chem. Biol.* **2021**, *61*, 32–42.
- [104] S. Learte-Aymamí, C. Vidal, A. Gutiérrez-González, J. L. Mascareñas, *Angew. Chem. Int. Ed.* **2020**, *59*, 9149–9154.
- [105] U. Prabhakar, H. Maeda, R. K. Jain, E. M. Sevick-Muraca, W. Zamboni, O. C. Farokhzad, S. T. Barry, A. Gabizon, P. Piotr Grodzinski, D. C. Blakey, *Cancer Res.* **2013**, *73*, 2412–2418.
- [106] D. J. Gorin, F. D. Toste, *Nature* **2007**, *446*, 395–403.
- [107] A. Fürstner, P. W. Davies, *Angew. Chem. Int. Ed.* **2007**, *46*, 3410–3449; *Angew. Chem.* **2007**, *119*, 3478–3519.
- [108] F. López, J. L. Mascareñas, *Beilstein J. Org. Chem.* **2013**, *9*, 2250–2264.
- [109] K. Tsubokura, K. K. H. Vong, A. R. Pradipta, A. Ogura, S. Urano, T. Tahara, S. Nozaki, H. Onoe, Y. Nakao, R. Sibgatullina, et al., *Angew. Chem. Int. Ed.* **2017**, *56*, 3579–3584; *Angew. Chem.* **2017**, *129*, 3633–3638.
- [110] A. M. Pérez-López, B. Rubio-Ruiz, V. Sebastián, L. Hamilton, C. Adam, T. L. Bray, S. Irusta, P. M. Brennan, G. C. Lloyd-Jones, D. Sieger, et al., *Angew. Chem. Int. Ed.* **2017**, *56*, 12548–12552; *Angew. Chem.* **2017**, *129*, 12722–12726.
- [111] A. Sousa-Castillo, J. R. Couceiro, M. Tomás-Gamasa, A. Mariño-López, F. López, W. Baaziz, O. Ersen, M. Comesaña-Hermo, J. L. Mascareñas, M. A. Correa-Duarte, *Nano Lett.* **2020**, *20*, 7068–7076.
- [112] L. Schoonen, J. C. M. Van Hest, *Adv. Mater.* **2016**, *28*, 1109–1128.
- [113] A. Belluati, I. Craciun, C. E. Meyer, S. Rigo, C. G. Palivan, *Curr. Opin. Biotechnol.* **2019**, *60*, 53–62.
- [114] H. Che, J. C. M. van Hest, *ChemNanoMat* **2019**, *5*, 1092–1109.
- [115] M. Godoy-Gallardo, M. J. York-Duran, L. Hosta-Rigau, *Adv. Healthcare Mater.* **2018**, *7*, 1700917.
- [116] N. Ben-Haim, P. Broz, S. Marsch, W. Meier, P. Hunziker, *Nano Lett.* **2008**, *8*, 1368–1373.
- [117] P. Tanner, O. Onaca, V. Balasubramanian, W. Meier, C. G. Palivan, *Chem. Eur. J.* **2011**, *17*, 4552–4560.
- [118] P. Tanner, V. Balasubramanian, C. G. Palivan, *Nano Lett.* **2013**, *13*, 2875–2883.
- [119] T. Einfalt, D. Witzigmann, C. Edlinger, S. Sieber, R. Goers, A. Najer, M. Spulber, O. Onaca-Fischer, J. Huwyler, C. G. Palivan, *Nat. Commun.* **2018**, *9*, 1127.
- [120] V. Balasubramanian, O. Onaca, M. Ezhevskaya, S. Van Doorslaer, B. Sivasankaran, C. G. Palivan, *Soft Matter* **2011**, *7*, 5595–5603.
- [121] S. F. M. van Dongen, W. P. R. Verdurmen, R. J. R. W. Peters, R. J. M. Nolte, R. Brock, J. C. M. van Hest, *Angew. Chem. Int. Ed.* **2010**, *49*, 7213–7216; *Angew. Chem.* **2010**, *122*, 7371–7374.
- [122] Y. Zhang, N. Gal, F. Itel, I. N. Westensee, E. Brodzkij, D. Mayer, S. Stenger, M. Castellote-Borrell, T. Boesen, S. R. Tabaei, et al., *Nanoscale* **2019**, *11*, 11530–11541.
- [123] C. Ade, E. Brodzkij, B. Thingholm, N. Gal, F. Itel, E. Taipaleenmäki, M. J. Hviid, P. S. Schattling, B. Städler, *ACS Appl. Polym. Mater.* **2019**, *1*, 1532–1539.
- [124] L. M. P. E. Van Oppen, L. K. E. A. Abdelmohsen, S. E. Van Emst-De Vries, P. L. W. Welzen, D. A. Wilson, J. A. M. Smeitink, W. J. H. Koopman, R. Brock, P. H. G. M. Willems, D. S. Williams, et al., *ACS Cent. Sci.* **2018**, *4*, 917–928.
- [125] Y. Anraku, A. Kishimura, M. Kamiya, S. Tanaka, T. Nomoto, K. Toh, Y. Matsumoto, S. Fukushima, D. Sueyoshi, M. R. Kano, et al., *Angew. Chem. Int. Ed.* **2016**, *55*, 560–565; *Angew. Chem.* **2016**, *128*, 570–575.
- [126] T. Nishimura, Y. Sasaki, K. Akiyoshi, *Adv. Mater.* **2017**, *29*, 1702406.
- [127] S. Lee, H. Koo, J. H. Na, K. E. Lee, S. Y. Jeong, K. Choi, S. H. Kim, I. C. Kwon, K. Kim, *ACS Nano* **2014**, *8*, 4257–4267.
- [128] V. Chan, S. K. Novakowski, S. Law, C. Klein-Bosgoed, C. J. Kastrup, *Angew. Chem. Int. Ed.* **2015**, *54*, 13590–13593; *Angew. Chem.* **2015**, *127*, 13794–13797.
- [129] B. Stadler, R. Chandrawati, A. D. Price, S. F. Chong, K. Breheney, A. Postma, L. A. Connal, A. N. Zelikin, F. Caruso, *Angew. Chem. Int. Ed.* **2009**, *48*, 4359–4362; *Angew. Chem.* **2009**, *121*, 4423–4426.
- [130] B. Thingholm, P. Schattling, Y. Zhang, B. Städler, *Small* **2016**, *12*, 1806–1814.
- [131] M. Godoy-Gallardo, C. Labay, M. M. T. Jansman, P. K. Ek, L. Hosta-Rigau, *Adv. Healthcare Mater.* **2017**, *6*, 1601190.
- [132] M. Godoy-gallardo, V. D. Trikalitis, P. J. Kempen, J. B. Larsen, T. L. Andresen, L. Hosta-rigau, *ACS Appl. Mater. Interfaces* **2017**, *9*, 15907–15921.
- [133] A. Larrañaga, I. L. M. Isa, V. Patil, S. Thamboo, M. Lomora, M. A. Fernández-Yague, J. R. Sarasua, C. G. Palivan, A. Pandit, *Acta Biomater.* **2018**, *67*, 21–31.
- [134] M. J. York-Duran, M. Godoy-Gallardo, M. M. T. Jansman, L. Hosta-Rigau, *Biomater. Sci.* **2019**, *7*, 4813–4826.
- [135] S. A. Bode, I. J. Minten, R. J. M. Nolte, J. J. L. M. Cornelissen, *Nanoscale* **2011**, *3*, 2376–2389.
- [136] B. Maity, K. Fujita, T. Ueno, *Curr. Opin. Chem. Biol.* **2015**, *25*, 88–97.
- [137] S. Zhang, J. Zang, W. Wang, H. Chen, X. Zhang, F. Wang, H. Wang, G. Zhao, *Angew. Chem. Int. Ed.* **2016**, *55*, 16064–16070; *Angew. Chem.* **2016**, *128*, 16298–16304.
- [138] S. Zhang, J. Zang, X. Zhang, H. Chen, B. Mikami, G. Zhao, *ACS Nano* **2016**, *10*, 10382–10388.

- [139] C. R. Olsen, T. J. Smith, J. S. Embley, J. H. Maxfield, K. R. Hansen, J. R. Peterson, A. M. Henrichsen, S. D. Erickson, D. C. Buck, J. S. Colton, et al., *Nanotechnology* **2017**, *28*, 195601–195610.
- [140] K. W. Pulsipher, S. Honig, S. Deng, I. J. Dmochowski, *J. Inorg. Biochem.* **2017**, *174*, 169–176.
- [141] S. Kanbak-Aksu, M. Nahid Hasan, W. R. Hagen, F. Hollmann, D. Sordi, R. A. Sheldon, I. W. C. E. Arends, *Chem. Commun.* **2012**, *48*, 5745–5747.
- [142] X. Liu, W. Wei, Q. Yuan, X. Zhang, N. Li, Y. Du, G. Ma, C. Yan, D. Ma, *Chem. Commun.* **2012**, *48*, 3155–3157.
- [143] S. Tetter, D. Hilvert, *Angew. Chem. Int. Ed.* **2017**, *56*, 14933–14936; *Angew. Chem.* **2017**, *129*, 15129–15132.
- [144] S. Chakraborti, A. Korpi, M. Kumar, P. Stępień, M. A. Kostianen, J. G. Heddl, *Nano Lett.* **2019**, *19*, 3918–3924.
- [145] V. V. Shuvaev, M. Khoshnejad, K. W. Pulsipher, R. Y. Kiseleva, E. Arguiri, J. C. Cheung-Lau, K. M. LeFort, M. Christofidou-Solomidou, R. V. Stan, I. J. Dmochowski, et al., *Biomaterials* **2018**, *185*, 348–359.
- [146] A. Macone, S. Masciarelli, F. Palombarini, D. Quaglio, A. Boffi, M. C. Trabuco, P. Baiocco, F. Fazi, A. Bonamore, *Sci. Rep.* **2019**, *9*, 11749.
- [147] K. Renggli, M. G. Nussbaumer, R. Urbani, T. Pfohl, N. Bruns, *Angew. Chem. Int. Ed.* **2014**, *53*, 1443–1447; *Angew. Chem.* **2014**, *126*, 1467–1472.
- [148] K. Renggli, N. Sauter, M. Rother, M. G. Nussbaumer, R. Urbani, T. Pfohl, N. Bruns, *Polym. Chem.* **2017**, *8*, 2133–2136.
- [149] M. G. Nussbaumer, C. Bisig, N. Bruns, *Chem. Commun.* **2016**, *52*, 10537–10539.
- [150] X. Wang, H. Sun, C. Wang, *Anal. Bioanal. Chem.* **2019**, *411*, 3819–3827.
- [151] X. Wang, H. Sun, C. Liu, C. Wang, *Anal. Methods* **2019**, *11*, 2197–2203.
- [152] X. Wang, S. Li, C. Wang, C. J. Mujuni, T. Yue, F. Huang, *ACS Biomater. Sci. Eng.* **2020**, *6*, 833–841.
- [153] A. Ora, E. Järvihaavisto, H. Zhang, H. Auvinen, H. A. Santos, M. A. Kostianen, V. Linko, *Chem. Commun.* **2016**, *52*, 14161–14164.
- [154] S. Zhao, F. Duan, S. Liu, T. Wu, Y. Shang, R. Tian, J. Liu, Z.-G. Wang, Q. Jiang, B. Ding, *ACS Appl. Mater. Interfaces* **2019**, *11*, 11112–11118.
- [155] D. W. Urry, C. H. Luan, T. M. Parker, D. C. Gowda, K. U. Prasad, M. C. Reid, A. Safavy, *J. Am. Chem. Soc.* **1991**, *113*, 4346–4348.
- [156] D. W. Urry, *J. Phys. Chem. B* **1997**, *101*, 11007–11028.
- [157] S. Saha, S. Banskota, S. Roberts, N. Kirmani, A. Chilkoti, *Adv. Ther.* **2020**, *3*, 1900164.
- [158] A. Schreiber, L. G. Stühn, M. C. Huber, S. E. Geissinger, A. Rao, S. M. Schiller, *Small* **2019**, *15*, 1900163.
- [159] A. Schreiber, M. C. Huber, S. M. Schiller, *Langmuir* **2019**, *35*, 9593–9610.
- [160] M. C. Huber, A. Schreiber, S. M. Schiller, *ChemBioChem* **2019**, *20*, 2618–2632.
- [161] K. Vogele, T. Frank, L. Gasser, M. A. Goetzfried, M. W. Hackl, S. A. Sieber, F. C. Simmel, T. Pirzer, *Nat. Commun.* **2018**, *9*, 3862.
- [162] M. C. Huber, A. Schreiber, P. von Olshausen, B. R. Varga, O. Kretz, B. Joch, S. Barnert, R. Schubert, S. Eimer, P. Kele, et al., *Nat. Mater.* **2015**, *14*, 125–132.
- [163] S. Frank, A. D. Lawrence, M. B. Prentice, M. J. Warren, *J. Biotechnol.* **2013**, *163*, 273–279.
- [164] T. Li, Q. Jiang, J. Huang, C. M. Aitchison, F. Huang, M. Yang, G. F. Dykes, H.-L. He, Q. Wang, R. S. Sprick, et al., *Nat. Commun.* **2020**, *11*, 5448.
- [165] T. W. Giessen, P. A. Silver, *Nat. Microbiol.* **2017**, *2*, 17029.
- [166] M. Sutter, D. Boehringer, S. Gutmann, S. Günther, D. Prangishvili, M. J. Loessner, K. O. Stetter, E. Weber-Ban, N. Ban, *Nat. Struct. Mol. Biol.* **2008**, *15*, 939–947.
- [167] T. W. Giessen, *Curr. Opin. Chem. Biol.* **2016**, *34*, 1–10.
- [168] F. Sigmund, S. Pettinger, M. Kube, F. Schneider, M. Schifferer, S. Schneider, M. V. Efremova, J. Pujol-Martí, M. Aichler, A. Walch, et al., *ACS Nano* **2019**, *13*, 8114–8123.
- [169] T. W. Giessen, P. A. Silver, *ACS Synth. Biol.* **2016**, *5*, 1497–1504.
- [170] T. Lee, T. S. Carpenter, P. D'haeseleer, D. F. Savage, M. C. Yung, *Biotechnol. Bioeng.* **2020**, *117*, 603–613.
- [171] R. M. Putri, J. W. Fredy, J. J. L. M. Cornelissen, M. S. T. Koay, N. Katsonis, *ChemPhysChem* **2016**, *17*, 1815–1818.
- [172] R. Klem, M. V. De Ruiter, J. J. L. M. Cornelissen, *Mol. Pharm.* **2018**, *15*, 2991–2996.
- [173] E. M. Williams, S. M. Jung, J. L. Coffman, S. Lutz, *ACS Synth. Biol.* **2018**, *7*, 2514–2517.
- [174] W. F. Rurup, J. Snijder, M. S. T. Koay, A. J. R. Heck, J. J. L. M. Cornelissen, *J. Am. Chem. Soc.* **2014**, *136*, 3828–3832.
- [175] A. Tamura, Y. Fukutani, T. Takami, M. Fujii, Y. Nakaguchi, Y. Murakami, K. Noguchi, M. Yohda, M. Odaka, *Biotechnol. Bioeng.* **2015**, *112*, 13–20.
- [176] C. Cassidy-Amstutz, L. Oltrogge, C. C. Going, A. Lee, P. Teng, D. Quintanilla, A. East-Seletsky, E. R. Williams, D. F. Savage, *Biochemistry* **2016**, *55*, 3461–3468.
- [177] R. M. Putri, C. Allende-Ballester, D. Luque, R. Klem, K. Rousou, A. Liu, C. H.-H. Traulsen, W. F. Rurup, M. S. T. Koay, J. R. Castón, et al., *ACS Nano* **2017**, *11*, 12796–12804.
- [178] Y. H. Lau, T. W. Giessen, W. J. Altenburg, P. A. Silver, *Nat. Commun.* **2018**, *9*, 1311.
- [179] F. Sigmund, C. Massner, P. Erdmann, A. Stelzl, H. Rolbieski, M. Desai, S. Bricault, T. P. Wörner, J. Snijder, A. Geerlof, et al., *Nat. Commun.* **2018**, *9*, 1990.
- [180] Y. Azuma, T. G. W. Edwardson, D. Hilvert, *Chem. Soc. Rev.* **2018**, *47*, 3543–3557.
- [181] X. Han, K. J. Woycechowsky, *Biochemistry* **2017**, *56*, 6211–6220.
- [182] Q. Guo, G. C. Thomas, K. J. Woycechowsky, *RSC Adv.* **2017**, *7*, 34676–34686.
- [183] B. Wörsdörfer, Z. Pianowski, D. Hilvert, *J. Am. Chem. Soc.* **2012**, *134*, 909–911.
- [184] R. Zschoche, D. Hilvert, *J. Am. Chem. Soc.* **2015**, *137*, 16121–16132.
- [185] Y. Azuma, R. Zschoche, M. Tinzl, D. Hilvert, *Angew. Chem. Int. Ed.* **2016**, *55*, 1531–1534; *Angew. Chem.* **2016**, *128*, 1555–1558.
- [186] R. Frey, T. Hayashi, D. Hilvert, *Chem. Commun.* **2016**, *52*, 10423–10426.
- [187] R. Frey, S. Mantri, M. Rocca, D. Hilvert, *J. Am. Chem. Soc.* **2016**, *138*, 10072–10075.
- [188] E. Sasaki, D. Böhringer, M. Van De Waterbeemd, M. Leibundgut, R. Zschoche, A. J. R. Heck, N. Ban, D. Hilvert, *Nat. Commun.* **2017**, *8*, 14663.
- [189] Y. Azuma, M. Herger, D. Hilvert, *J. Am. Chem. Soc.* **2018**, *140*, 558–561.
- [190] T. Beck, S. Tetter, M. Künzle, D. Hilvert, *Angew. Chem. Int. Ed.* **2015**, *54*, 937–940; *Angew. Chem.* **2015**, *127*, 951–954.
- [191] F. P. Seebeck, K. J. Woycechowsky, W. Zhuang, J. P. Rabe, D. Hilvert, *J. Am. Chem. Soc.* **2006**, *128*, 4516–4517.
- [192] B. Worsdorfer, K. J. Woycechowsky, D. Hilvert, *Science* **2011**, *331*, 589–592.
- [193] M. Comellas-Aragonès, H. Engelkamp, V. I. Claessen, N. A. J. M. Sommerdijk, A. E. Rowan, P. C. M. Christianen, J. C. Maan, B. J. M. Verduin, J. J. L. M. Cornelissen, R. J. M. Nolte, *Nat. Nanotechnol.* **2007**, *2*, 635–639.
- [194] I. J. Minten, L. J. A. Hendriks, R. J. M. Nolte, J. J. L. M. Cornelissen, *J. Am. Chem. Soc.* **2009**, *131*, 17771–17773.
- [195] W. F. Rurup, F. Verbij, M. S. T. Koay, C. Blum, V. Subramaniam, J. J. L. M. Cornelissen, *Biomacromolecules* **2014**, *15*, 558–563.
- [196] L. Schoonen, R. J. M. Nolte, J. C. M. van Hest, *Nanoscale* **2016**, *14*, 14467–14472.
- [197] M. Brasch, R. M. Putri, M. V. de Ruiter, D. Luque, M. S. T. Koay, J. R. Castón, J. J. L. M. Cornelissen, *J. Am. Chem. Soc.* **2017**, *139*, 1512–1519.
- [198] M. B. Van Eldijk, J. C.-Y. Wang, I. J. Minten, C. Li, A. Zlotnick, R. J. M. Nolte, J. J. L. M. Cornelissen, J. C. M. Van Hest, *J. Am. Chem. Soc.* **2012**, *134*, 18506–18509.
- [199] L. Schoonen, R. J. M. Maas, R. J. M. Nolte, J. C. M. van Hest, *Tetrahedron* **2017**, *73*, 4968–4971.
- [200] S. B. P. E. Timmermans, D. F. M. Vervoort, L. Schoonen, R. J. M. Nolte, J. C. M. van Hest, *Chem. Asian J.* **2018**, *13*, 3518–3525.
- [201] X. Sun, Z. Cui, *Adv. Ther.* **2020**, *3*, 1900194.
- [202] J. D. Fiedler, S. D. Brown, J. L. Lau, M. G. Finn, *Angew. Chem. Int. Ed.* **2010**, *49*, 9648–9651; *Angew. Chem.* **2010**, *122*, 9842–9845.
- [203] J. D. Fiedler, M. R. Fishman, S. D. Brown, J. Lau, M. G. Finn, *Biomacromolecules* **2018**, *19*, 3945–3957.
- [204] S. Das, L. Zhao, K. Eloffson, M. G. Finn, *Biochemistry* **2020**, *59*, 2870–2881.
- [205] S. D. Brown, J. D. Fiedler, M. G. Finn, *Biochemistry* **2009**, *48*, 11155–11157.
- [206] J. E. Glasgow, S. L. Capehart, M. B. Francis, D. Tullman-Ercek, *ACS Nano* **2012**, *6*, 8658–8664.
- [207] J. E. Glasgow, M. A. Asensio, C. M. Jakobson, M. B. Francis, D. Tullman-Ercek, *ACS Synth. Biol.* **2015**, *4*, 1011–1019.
- [208] T. W. Giessen, P. A. Silver, *ChemBioChem* **2016**, *17*, 1931–1935.
- [209] B. Zakeri, J. O. Fierer, E. Celik, E. C. Chittock, U. Schwarz-Linek, V. T. Moy, M. Howarth, *Proc. Natl. Acad. Sci. USA* **2012**, *109*, E690–E697.
- [210] D. P. Patterson, P. E. Prevelige, T. Douglas, *ACS Nano* **2012**, *6*, 5000–5009.
- [211] D. P. Patterson, B. Schwarz, K. El-Boubbou, J. van der Oost, P. E. Prevelige, T. Douglas, *Soft Matter* **2012**, *8*, 10158–10166.

- [212] P. C. Jordan, D. P. Patterson, K. N. Saboda, E. J. Edwards, H. M. Miettinen, G. Basu, M. C. Thielges, T. Douglas, *Nat. Chem.* **2015**, *8*, 179–185.
- [213] D. Patterson, E. Edwards, T. Douglas, *Isr. J. Chem.* **2015**, *55*, 96–101.
- [214] D. P. Patterson, B. Schwarz, R. S. Waters, T. Gedeon, T. Douglas, *ACS Chem. Biol.* **2014**, *9*, 359–365.
- [215] A. O'Neil, C. Reichhardt, B. Johnson, P. E. Prevelige, T. Douglas, *Angew. Chem. Int. Ed.* **2011**, *50*, 7425–7428; *Angew. Chem.* **2011**, *123*, 7563–7566.
- [216] H. K. Waghvani, M. Uchida, C.-Y. Fu, B. LaFrance, J. Sharma, K. McCoy, T. Douglas, *Biomacromolecules* **2020**, *21*, 2060–2072.
- [217] E. Selivanovitch, R. Koliyatt, T. Douglas, *Biomacromolecules* **2019**, *20*, 389–400.
- [218] R. Kant, A. Llauro, V. Rayaprolu, S. Qazi, P. J. de Pablo, T. Douglas, B. Bothner, *Biochim. Biophys. Acta Gen. Subj.* **2018**, *1862*, 1492–1504.
- [219] J. Sharma, M. Uchida, H. M. Miettinen, T. Douglas, *Nanoscale* **2017**, *9*, 10420–10430.
- [220] K. McCoy, E. Selivanovitch, D. Luque, B. Lee, E. Edwards, J. R. Castón, T. Douglas, *Biomacromolecules* **2018**, *19*, 3738–3746.
- [221] J. Sharma, T. Douglas, *Nanoscale* **2020**, *12*, 336–346.
- [222] T. O. Yeates, J. E. Padilla, *Curr. Opin. Struct. Biol.* **2002**, *12*, 464–470.
- [223] F. Lapenta, R. Jerala, *Curr. Opin. Struct. Biol.* **2020**, *63*, 90–96.
- [224] Y. Hsia, J. B. Bale, S. Gonen, D. Shi, W. Sheffler, K. K. Fong, U. Nattermann, C. Xu, P. S. Huang, R. Ravichandran, et al., *Nature* **2016**, *535*, 136–139.
- [225] Y.-T. Lai, D. Cascio, T. O. Yeates, *Science* **2012**, *336*, 1129–1129.
- [226] H. Li, G. Zheng, S. Zhu, *Microb. Cell Fact.* **2018**, *17*, 26.
- [227] J. B. Bale, S. Gonen, Y. Liu, W. Sheffler, D. Ellis, C. Thomas, D. Cascio, T. O. Yeates, T. Gonen, N. P. King, et al., *Science* **2016**, *353*, 389–394.
- [228] K. A. Cannon, R. U. Park, S. E. Boyken, U. Nattermann, S. Yi, D. Baker, N. P. King, T. O. Yeates, *Protein Sci.* **2020**, *29*, 919–929.
- [229] J. E. Padilla, C. Colovos, T. O. Yeates, *Proc. Natl. Acad. Sci. USA* **2001**, *98*, 2217–2221.
- [230] N. P. King, W. Sheffler, M. R. Sawaya, B. S. Vollmar, J. P. Sumida, I. Andre, T. Gonen, T. O. Yeates, D. Baker, *Science* **2012**, *336*, 1171–1174.
- [231] N. P. King, J. B. Bale, W. Sheffler, D. E. Mcnamara, S. Gonen, T. Gonen, T. O. Yeates, *Nature* **2014**, *510*, 103–108.
- [232] K. A. Cannon, V. N. Nguyen, C. Morgan, T. O. Yeates, *ACS Synth. Biol.* **2020**, *9*, 517–524.
- [233] A. S. Cristie-David, P. Koldewey, B. A. Meinen, J. C. A. Bardwell, E. N. G. Marsh, *Protein Sci.* **2018**, *27*, 1893–1900.
- [234] S. Badiyan, A. Sciore, J. D. Eschweiler, P. Koldewey, A. S. Cristie-david, B. T. Ruotolo, J. C. A. Bardwell, M. Su, E. N. G. Marsh, *ChemBioChem* **2017**, *18*, 1888–1892.
- [235] A. Sciore, M. Su, P. Koldewey, J. D. Eschweiler, K. A. Diffley, B. M. Linhares, B. T. Ruotolo, J. C. A. Bardwell, G. Skiniotis, E. N. G. Marsh, *Proc. Natl. Acad. Sci. USA* **2016**, *113*, 8681–8686.
- [236] D. P. Patterson, A. M. Desai, M. M. B. Holl, E. N. G. Marsh, *RSC Adv.* **2011**, *1*, 1004–1012.
- [237] D. P. Patterson, M. Su, T. M. Franzmann, A. Sciore, G. Skiniotis, E. N. G. Marsh, *Protein Sci.* **2014**, *23*, 190–199.
- [238] S. A. McConnell, K. A. Cannon, C. Morgan, R. McAllister, B. R. Amer, R. T. Clubb, T. O. Yeates, *ACS Synth. Biol.* **2020**, *9*, 381–391.
- [239] A. Ljubetič, F. Lapenta, H. Gradišar, I. Drobna, J. Aupič, Ž. Strmšek, D. Lainšček, I. Hafner-Bratkovič, A. Majerle, N. Krivec, et al., *Nat. Biotechnol.* **2017**, *35*, 1094–1101.
- [240] H. Gradišar, S. Božič, T. Doles, D. Vengust, I. Hafner-bratkovič, A. Mertelj, B. Webb, A. Šali, S. Klavžar, R. Jerala, *Nat. Chem. Biol.* **2013**, *9*, 362–366.
- [241] N. C. Seeman, *Annu. Rev. Biochem.* **2010**, *79*, 65–87.
- [242] J. N. Wright, W. L. Wong, J. A. Harvey, J. A. Garnett, L. S. Itzhaki, E. R. G. Main, *Structure* **2019**, *27*, 776–784.
- [243] J. Zang, H. Chen, X. Zhang, C. Zhang, J. Guo, M. Du, G. Zhao, *Nat. Commun.* **2019**, *10*, 778.
- [244] L. A. Campos, R. Sharma, S. Alvira, F. M. Ruiz, B. Ibarra-Molero, M. Sadqi, C. Alfonso, G. Rivas, J. M. Sanchez-Ruiz, A. Romero Garrido, et al., *Nat. Commun.* **2019**, *10*, 5703.
- [245] E. Golub, R. H. Subramanian, J. Esselborn, R. G. Alberstein, J. B. Bailey, J. A. Chiong, X. Yan, T. Booth, T. S. Baker, F. A. Tezcan, *Nature* **2020**, *578*, 172–176.
- [246] B. D. Weitzner, Y. Kipnis, A. G. Daniel, D. Hilvert, D. Baker, *Protein Sci.* **2019**, *28*, 2036–2041.
- [247] K. Chen, F. H. Arnold, *Nat. Catal.* **2020**, *3*, 203–213.

---

Manuscript received: December 16, 2020  
Revised manuscript received: January 15, 2021  
Accepted manuscript online: January 15, 2021  
Version of record online: March 4, 2021